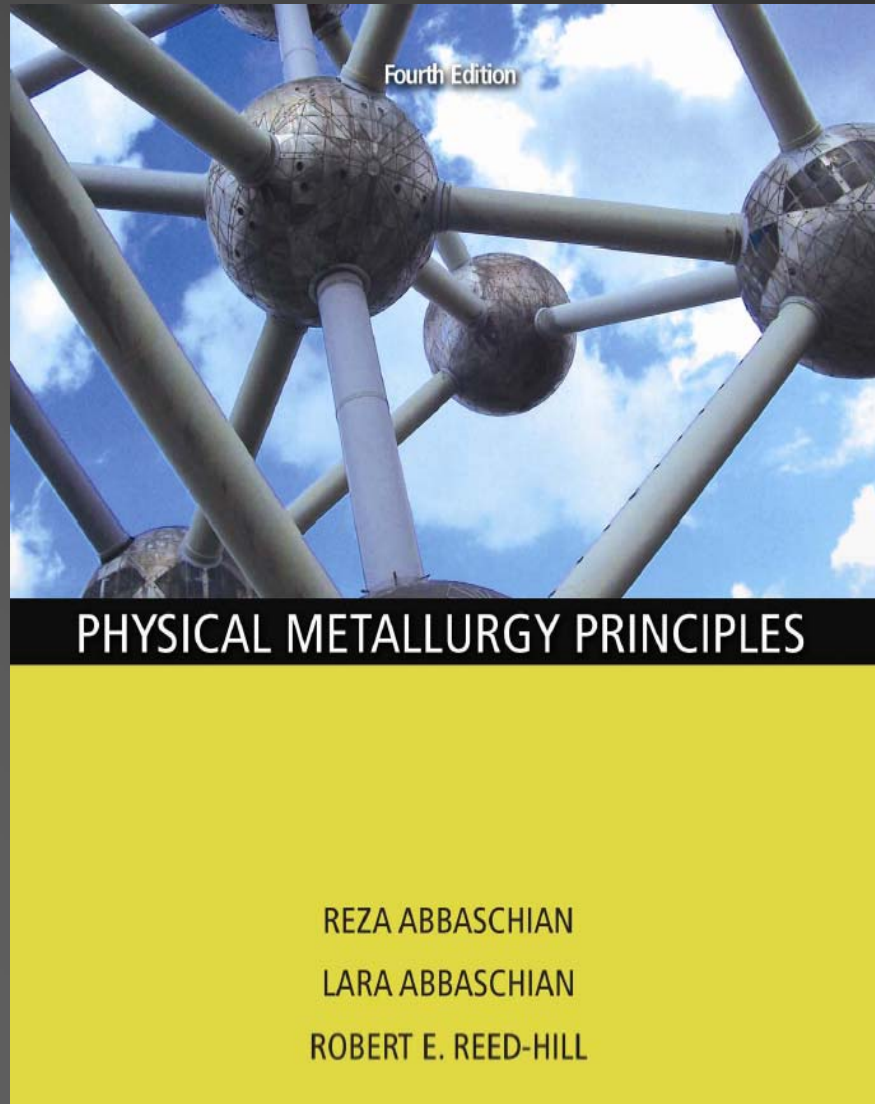


Physical Metallurgy Principles

Fourth

SI Version



Chapter Five:

Dislocations and Plastic Deformations

Connected with the relation of dislocations to plastic deformation

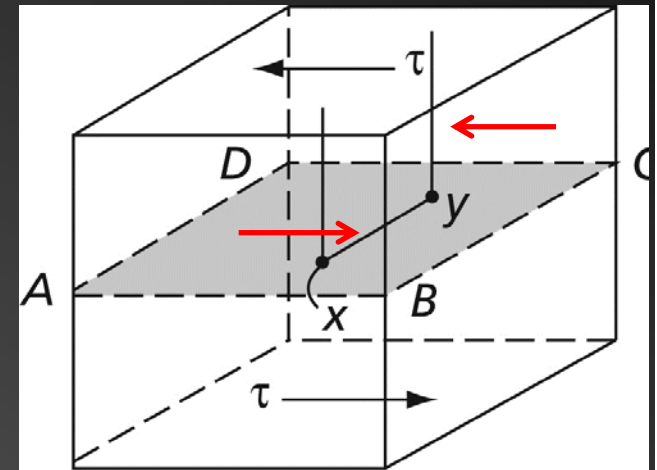
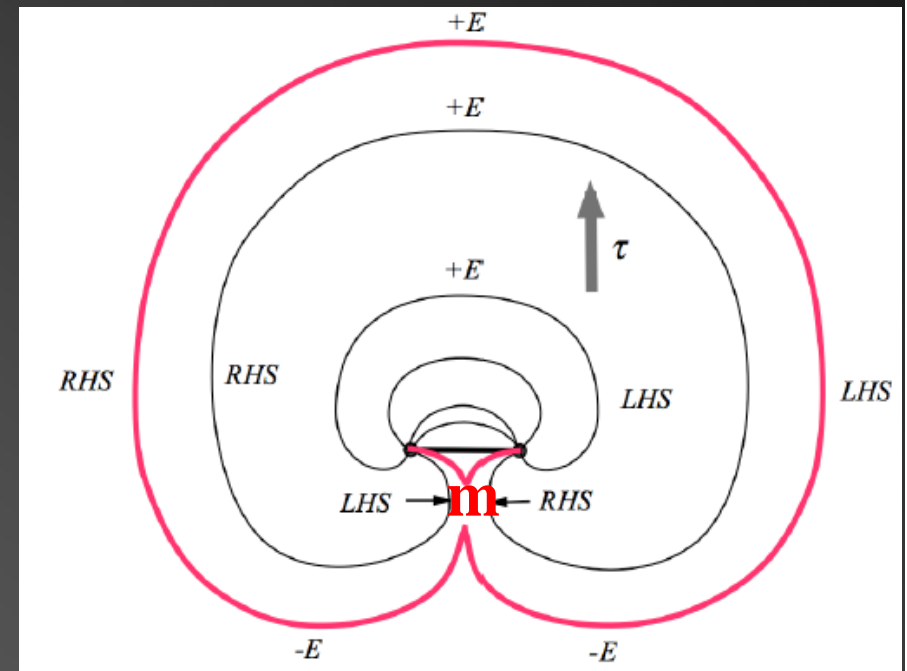
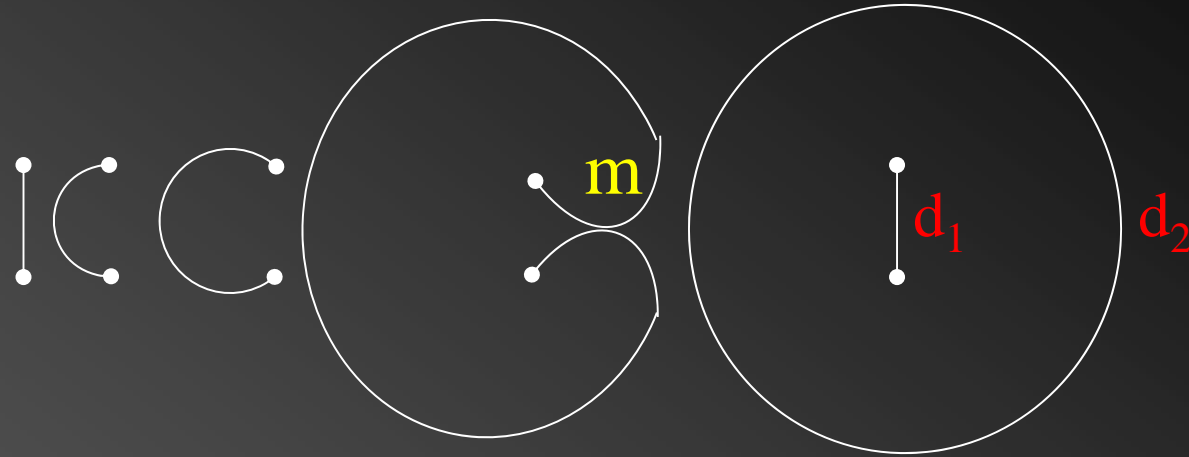


FIG. 5.1 Frank-Read source. The dislocation segment xy may move in plane $ABCD$ under the applied stress. Its ends, x and y , however, are fixed



5.2 Nucleation of Dislocations

- Dislocations can also be formed without the aid of Frank-Read or similar sources.

- Metal is not suitable for the dislocation nucleation studies

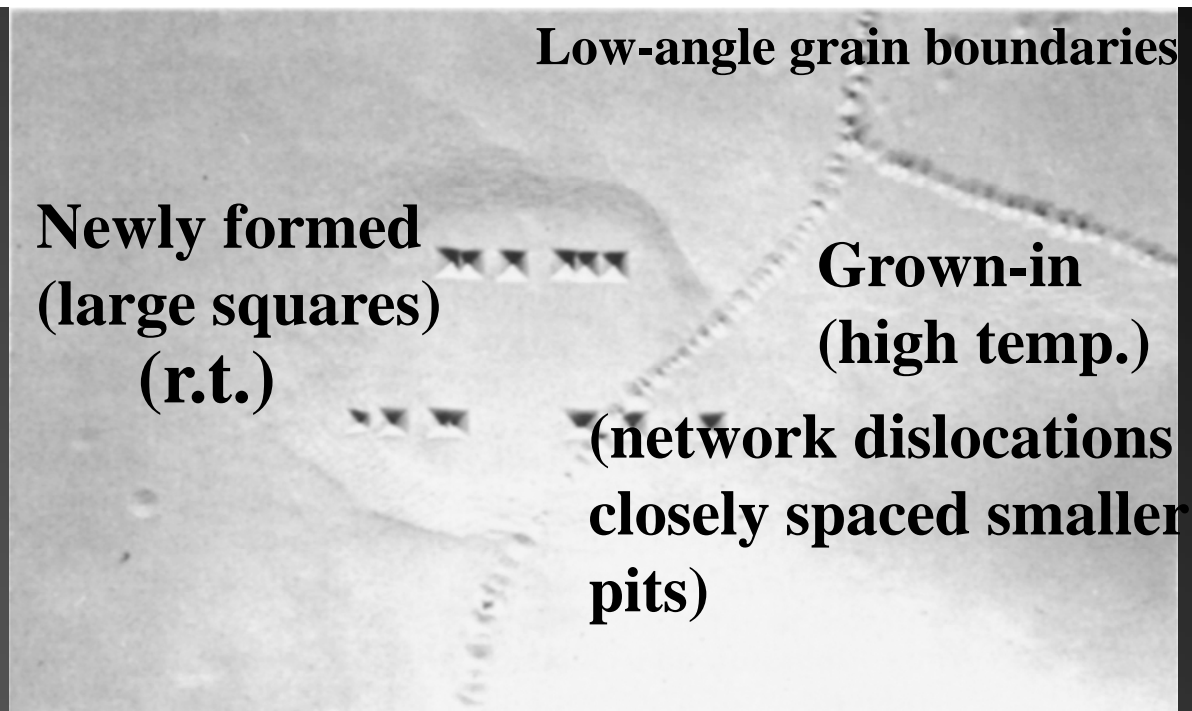


FIG. 5.3 The large square etched pits in horizontal rows correspond to dislocations formed in LiF at room temperature, while the smaller, closely spaced pits lying in curved rows were grown into the crystal when it was manufactured (Gilman, J. J., and Johnson, W. G., *Dislocations and Mechanical Properties of Crystals*, p. 116, John Wiley and Sons, Inc., New York, 1957. Used by permission of the author.)

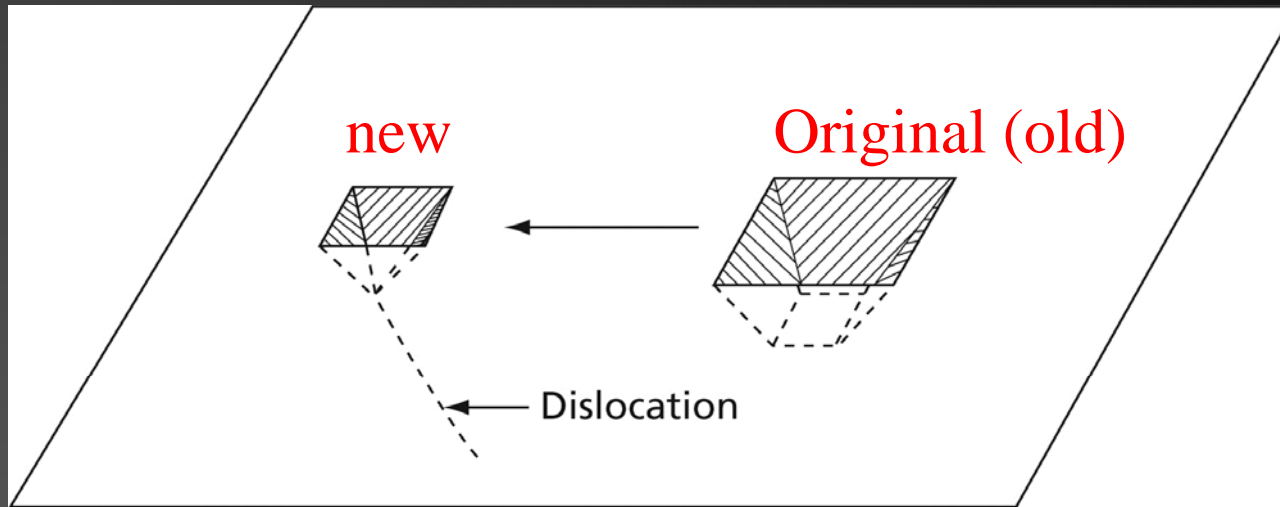
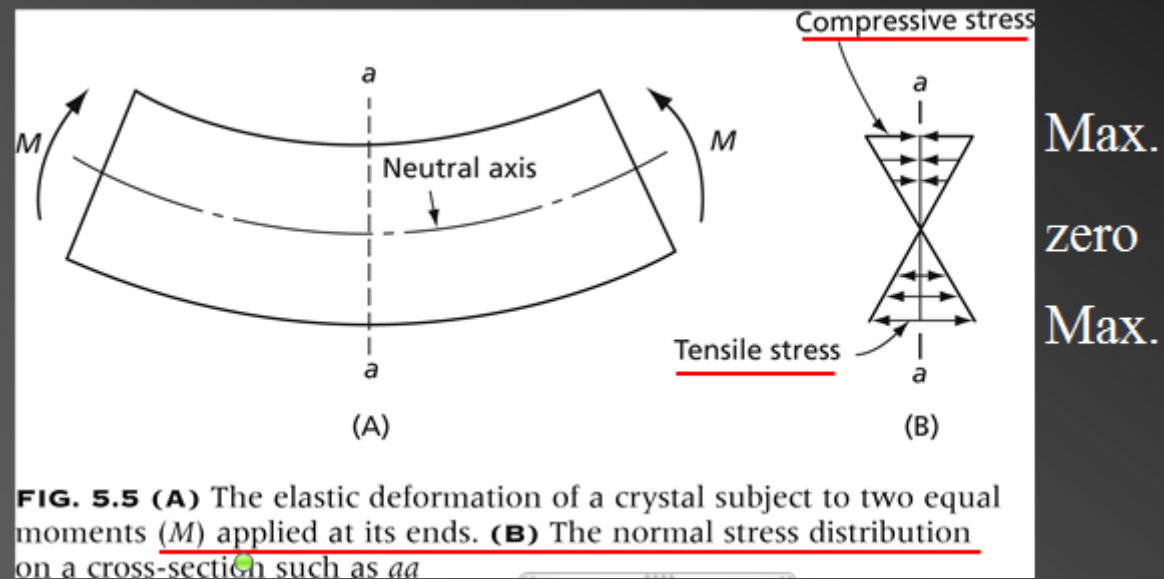


FIG. 5.4 Dislocation movement in LiF as revealed by repeated etching (Reprinted with permission from J.J. Gilman and W.G. Johnson, *Journal of Applied Physics*, Vol. 30, Issue 2, Page 129, Copyright 1959, American Institute of Physics)

5.3 Bend Gliding:



- The stress distribution: $\sigma_x = \frac{My}{I}$

M : bending moment
 y : vertical distance
 I : moment of inertia
 $(= \pi r^4/4$; for a circular rod)

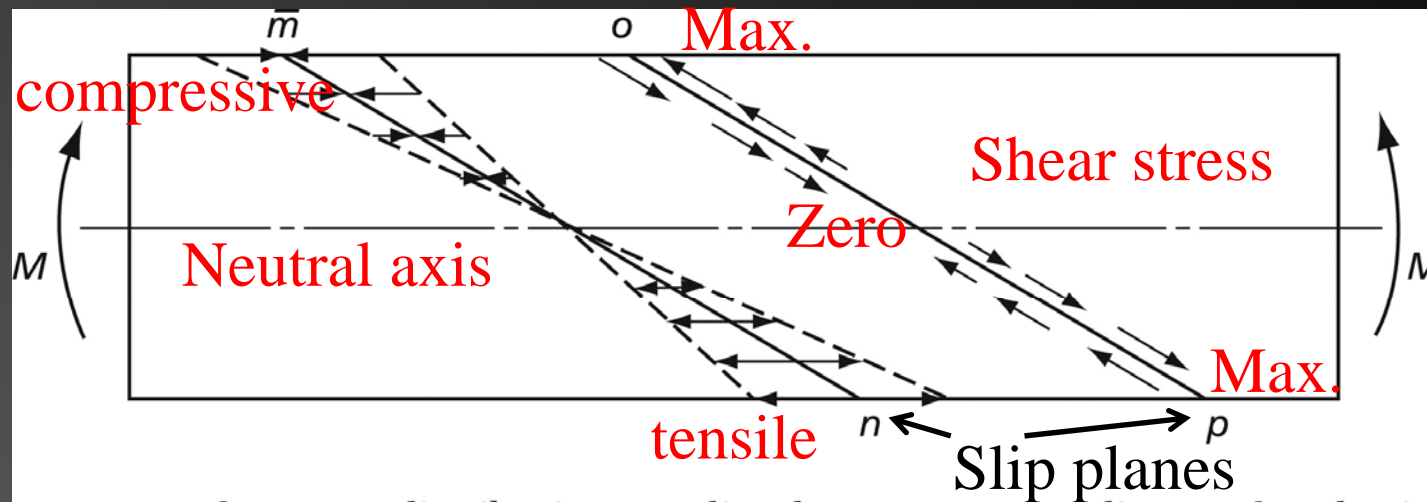


FIG. 5.6 The stress distribution on slip planes corresponding to the elastic deformation shown in Fig. 5.5

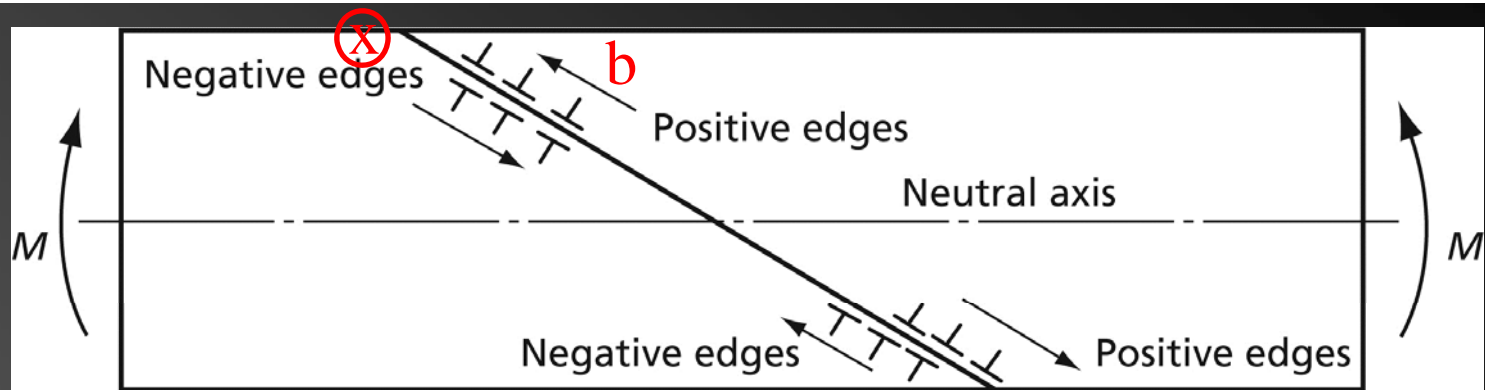


FIG. 5.7 The effect of the stress distribution on the movement of dislocations. Positive-edge components move toward the surface; negative edges toward the neutral axis

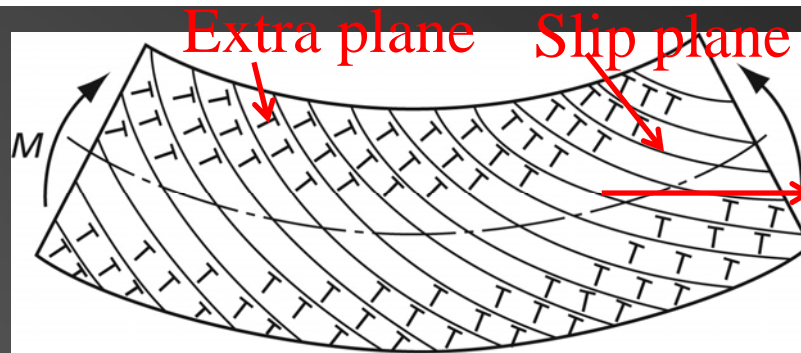


FIG. 5.8 Distribution of the excess edge dislocations in a plastically bent crystal

Narrow section surrounding the axis:
free of dislocations

=> under moderate stresses (not plastic)

=> will not be stressed above the elastic limit

5.4 Rotational Slip:

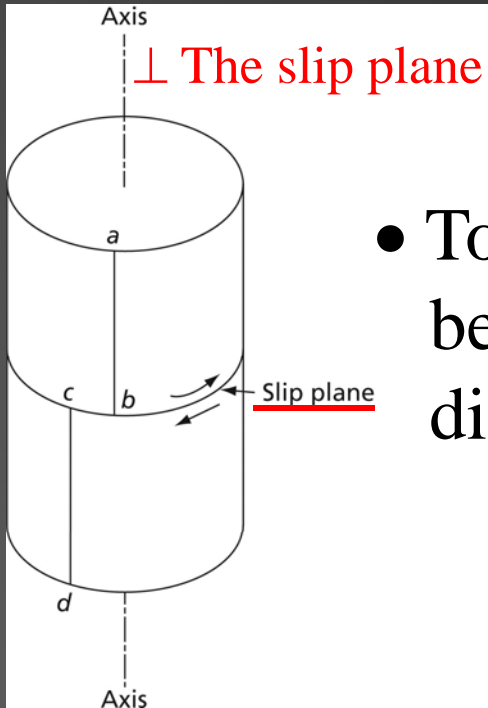
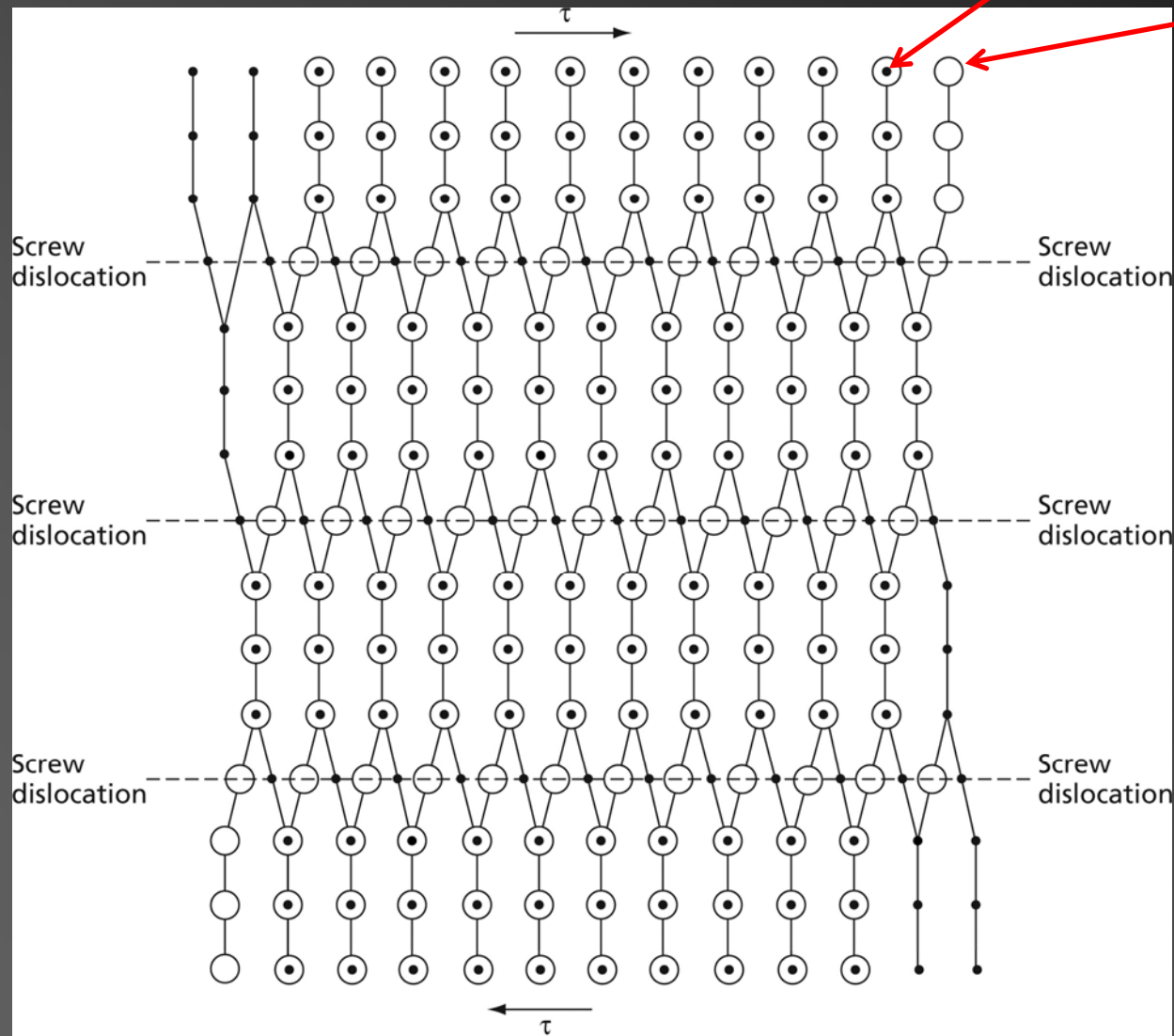


FIG. 5.9 A single crystal can be rotated about an axis normal to a slip plane that contains several slip directions

- Torsional deformation such as this can be explained in terms of screw dislocations lying on the slip plane.



Atoms just below
the slip plane.

Atoms just above
the slip plane.

FIG. 5.10 An array of parallel screw dislocations. Open circles represent atoms just above the slip plane, while dots correspond to atoms just below it

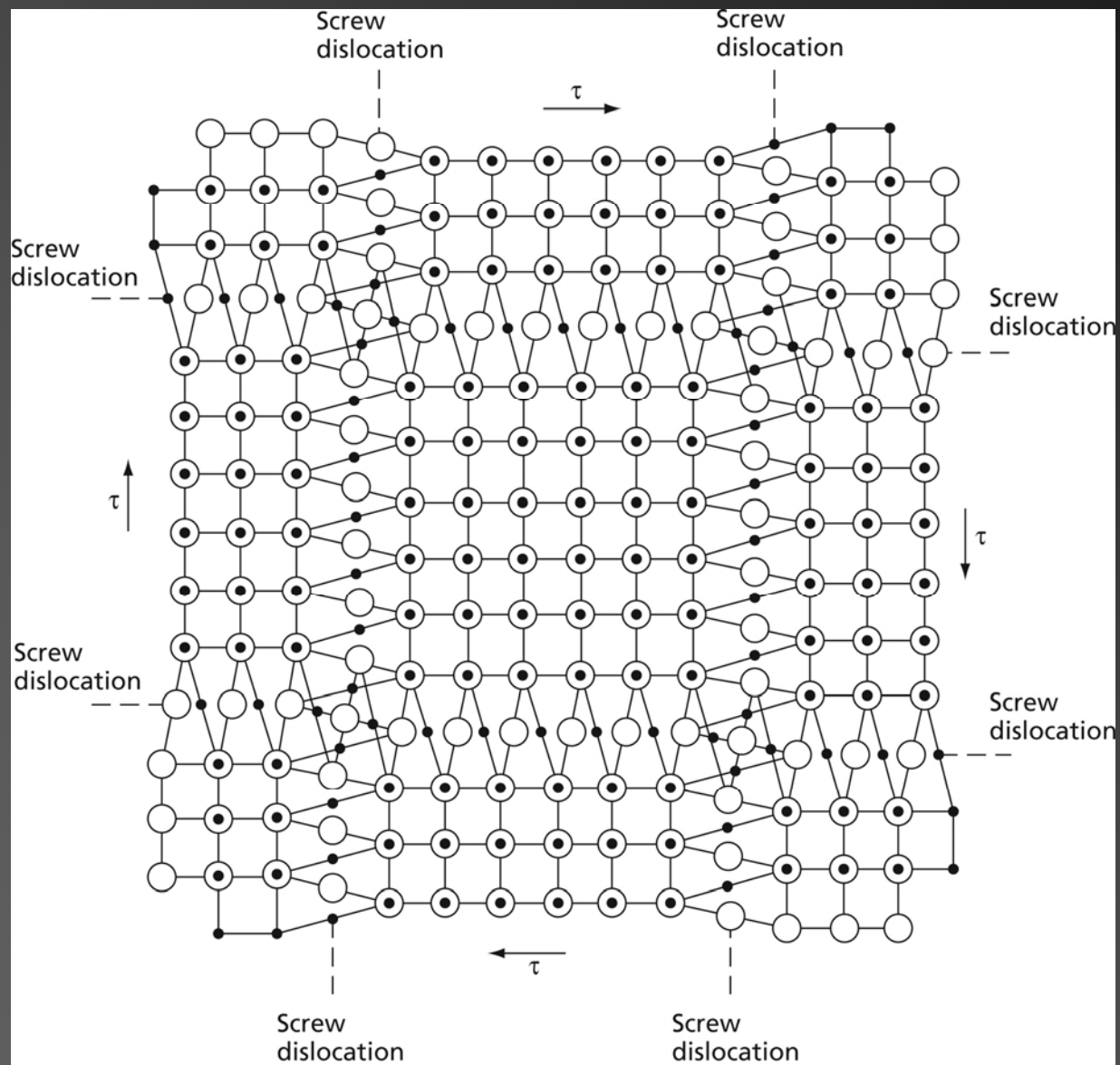
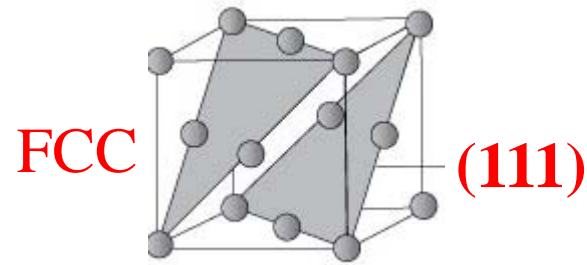


FIG. 5.11 A double array of screw dislocations. This array does not have a long-range strain field; open circles show atoms above the slip plane, while dots represent those below the plane

5.5 Slip Planes and Slip Directions

- Experimental fact: slip occurs preferentially on planes of **high atomic density**



mn: close packed direction

qr: not

Burgers vector

Burgers vector

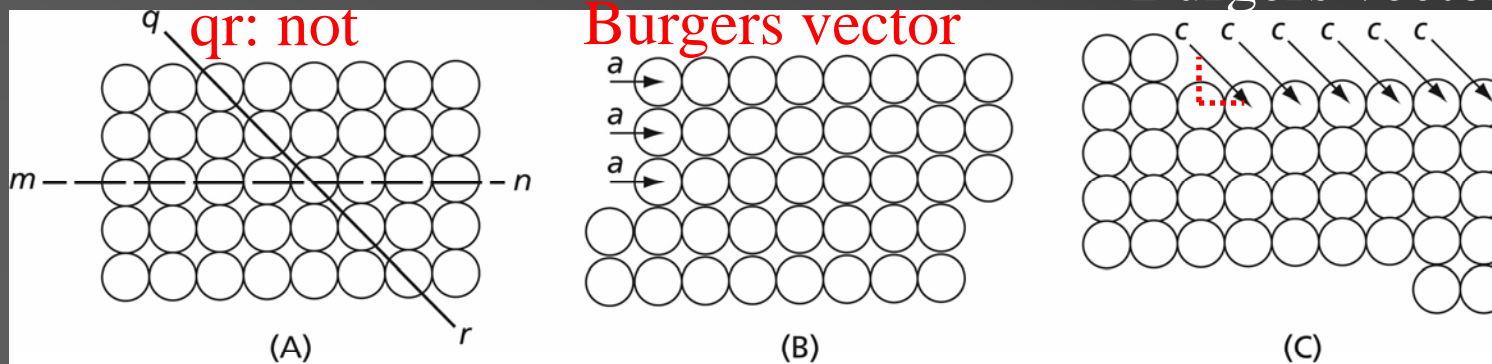


FIG. 5.12 Two ways in which a simple cubic lattice can be sheared while still maintaining the lattice symmetry: **(A)** Crystal before shearing, **(B)** shear in a close-packed direction, and **(C)** shear in a non-close-packed direction

- Strain energy $w = (\mu b^2/4\pi)\ln(r'/r)$

screw

$$W_s = \frac{\mu b^2}{4\pi} \ln\left(\frac{r'}{r_0}\right)$$

edge

$$W_s = \frac{\mu b^2}{4\pi(1-\nu)} \ln \frac{r'}{r_0}$$

mn: close packed direction

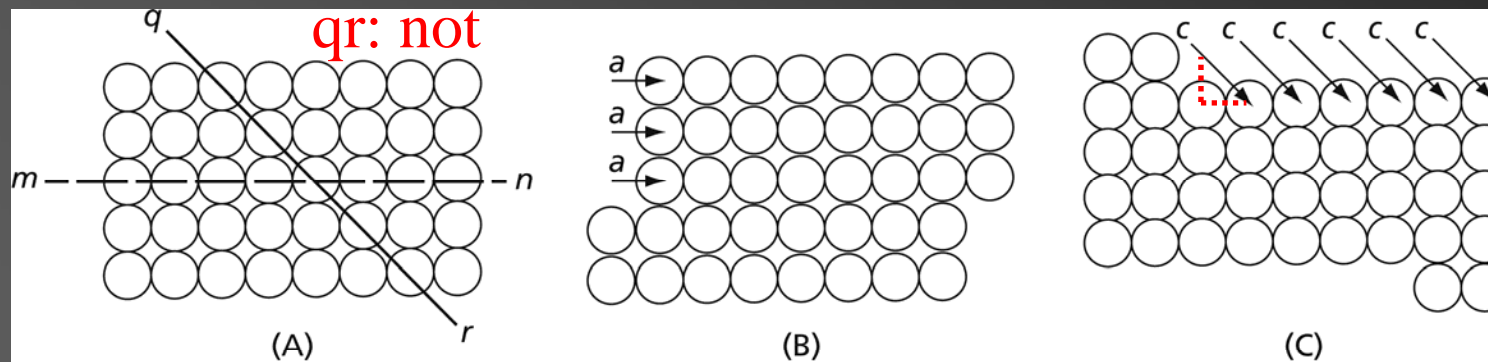


FIG. 5.12 Two ways in which a simple cubic lattice can be sheared while still maintaining the lattice symmetry: **(A)** Crystal before shearing, **(B)** shear in a close-packed direction, and **(C)** shear in a non-close-packed direction

5.6 Slip Systems:

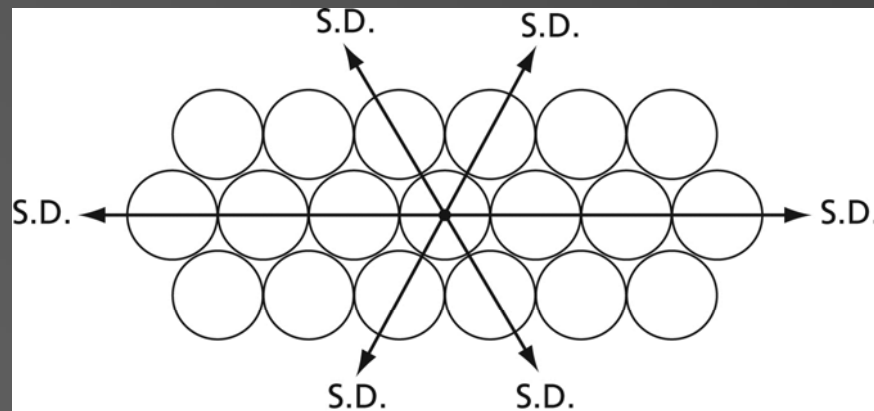


FIG. 5.13 The three slip directions (S.D.) in a plane of closest packing. Notice that this type of plane occurs in both the hexagonal close-packed and the face-centered cubic lattices

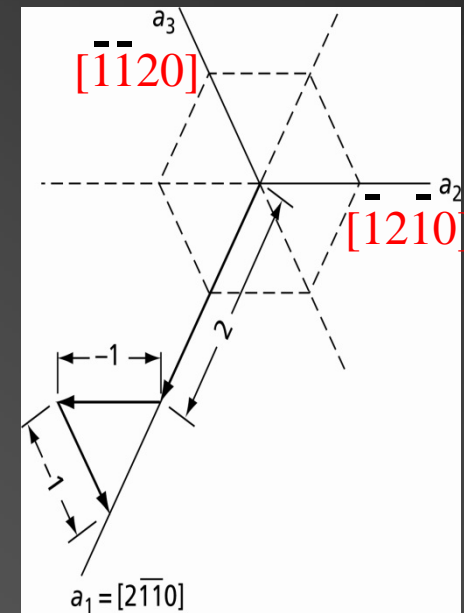


FIG. 1.18 Determination of indices of a digonal axis of Type I— $[2\bar{1}10]$

5.7 Critical Resolved Shear Stress (yield stress)

$$A_n = A_{sp} \cos \theta$$

A_n : cross section area perpendicular to the specimen axis

A_{sp} : the slip plane

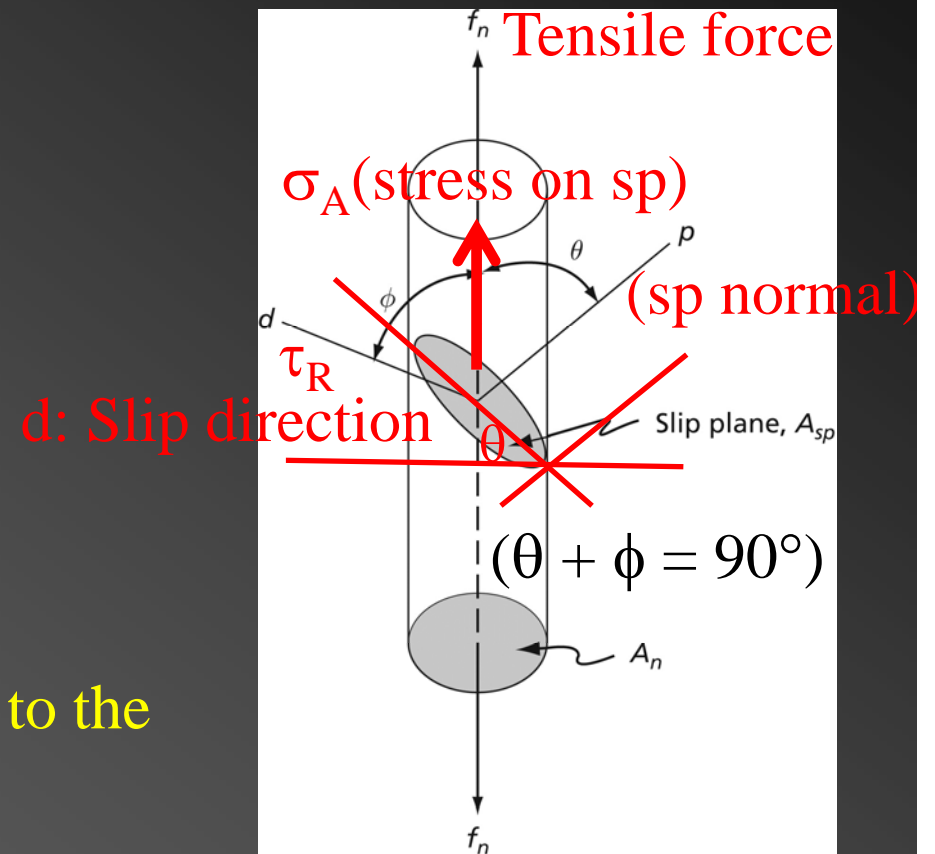


FIG. 5.14 A figure for the determination of the critical resolved shear stress equation

$$\tau_R = \frac{f_n \cos\phi}{A_{sp}} = \sigma_A \cos\phi = \frac{f_n \cos\phi}{\frac{A_n}{\cos\theta}} \quad (A_n = A_{sp} \cos\theta)$$

$$= \frac{f_n}{A_n} \cos\theta \cos\phi = \sigma \cos\theta \cos\phi : \text{Schmid's law}$$

τ_R : resolved shear stress (**shear stress on the slip plane in the slip direction**)

σ_A : the stress on the slip plane (A_{sp}), in the direction of f_n

σ : f_n/A_n , the normal tensile stress on A_n

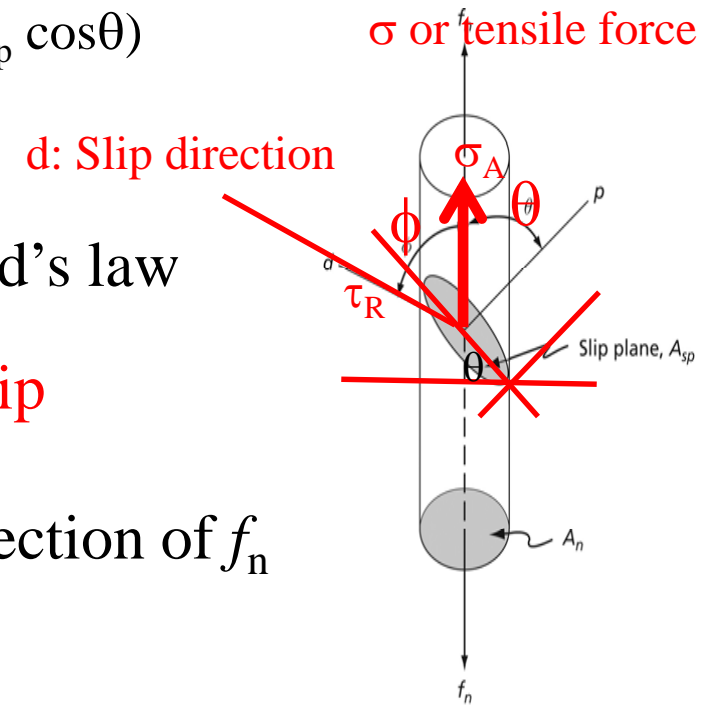
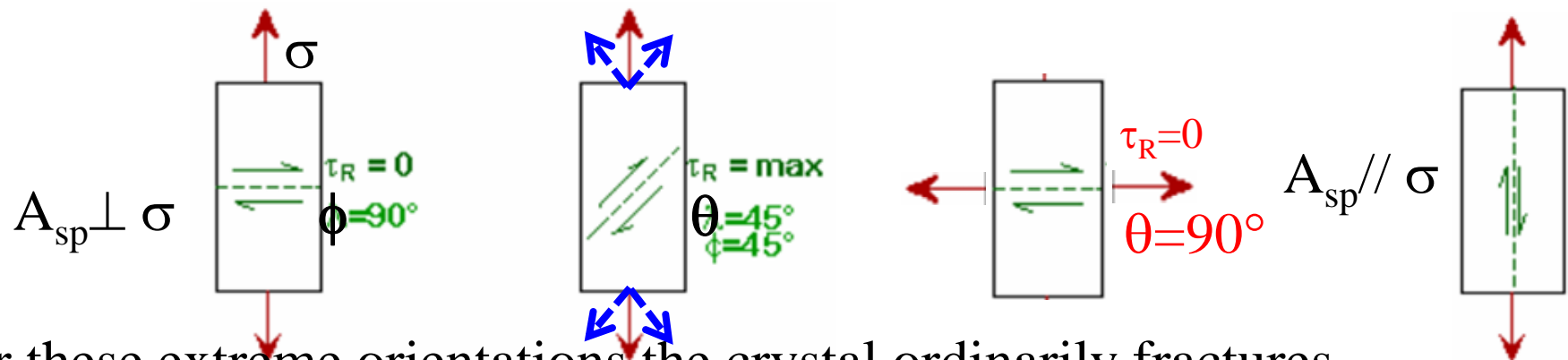


FIG. 5.14 A figure for the determination of the critical resolved shear stress equation



- For these extreme orientations the crystal ordinarily fractures rather than deforming plastically.

$$\tau_R = \sigma \cos\theta \cos\phi : \text{Schmid's law}$$

- Maximum shear stress (0.5σ) occurs when $\phi = \theta = 45^\circ$.

- if $\tau_R > \tau_{\text{crss}}$ (**critical resolved shear stress**)
=> plastic deformation by slip.

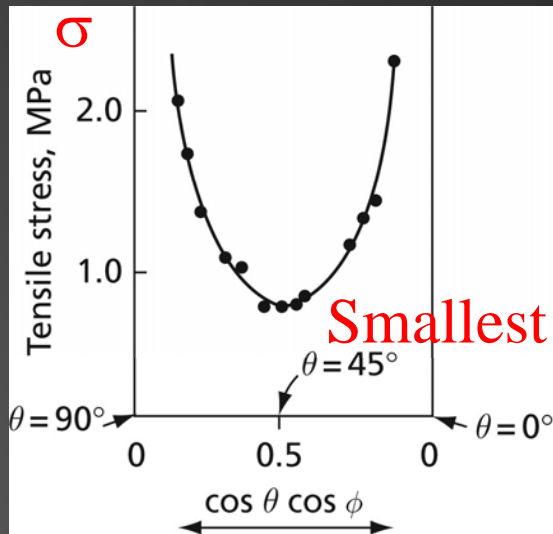


FIG. 5.15 The tensile yield point for magnesium single crystals of different orientations. Abscissae are values of the function $\cos \theta \cos \phi$. Smooth curve is for an assumed constant critical resolved shear stress of 63 psi (Burke, E. C., and Hibbard, W. R., Jr., *Trans. AIME*, **194**, 295 [1952].)

Smallest σ to get τ_{crss}

$$\tau_{\text{crss}} (\text{fixed}) = \sigma \cos \theta \cos \phi$$

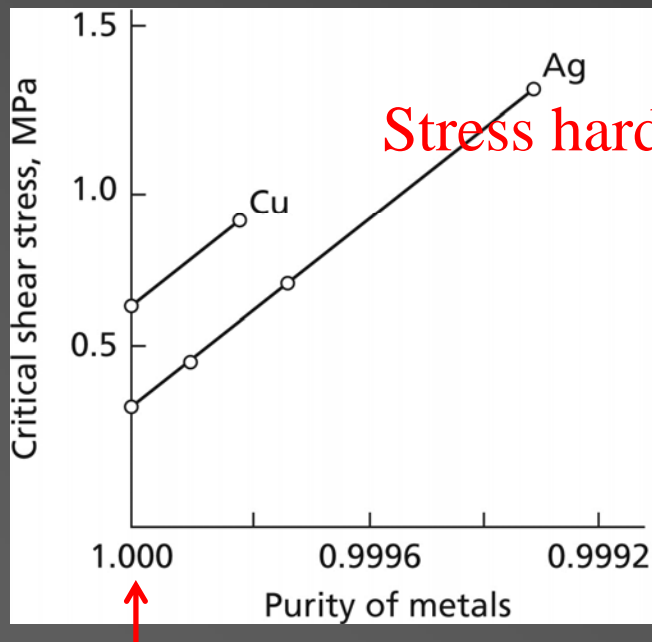
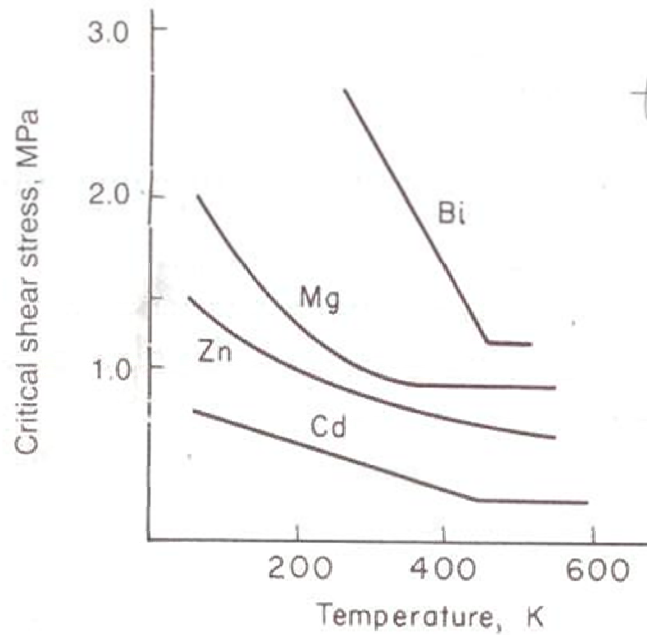


FIG. 5.16 Variation of the critical resolved shear stress with purity of the metal (After Rosi, F. D., *Trans. AIME*, **200**, 1009 [1954].)

Stress hardening

Totally pure metals: very high τ_R



temp. $\downarrow \Rightarrow$ critical shear stress \uparrow

Fig. 5.17 Effect of temperature on the critical shear stress. *Note:* The data on which these curves are based predate those of Table 5.2. The higher critical stresses in this case correspond to crystals of lower purity. (Schmid, E., and Boas, W., *Kristallplastizität*, Julius Springer, Berlin, 1935.)

h.t. very high

- **Strengthening of metallic materials:**

- There are five main strengthening mechanisms for metals

- 1. Work hardening**

⇒ such as beating a red-hot piece of metal on anvil, has been used for centuries by blacksmiths to introduce dislocations into materials, increasing their yield strengths.

2. Solid Solution Strengthening/Alloying (impurity)

3. Precipitation Hardening (impurity)

4. Grain Boundary (Grain Size) Strengthening

5. Transformation Hardening

5.8 Slip On Equivalent Slip Systems

5.9 The Dislocation Density

- Dislocation density (ρ) :
 1. by estimating the length of the dislocation line (cm/cm^3)
 2. by the number of dislocation etch pits ($\#/\text{cm}^2$).

5.10 Slip Systems in Different Crystal Forms

Slip Systems in FCC:

- close packed direction: $\langle 110 \rangle$; four closed packed planes (octahedral plane): (111) , $(\bar{1}11)$, $(1\bar{1}1)$, $(11\bar{1})$; Each octahedral plane have three slip directions
 $\Rightarrow 4 \times 3 = 12$ slip systems.

- **If the slip planes intersecting each other, or mutual interference of dislocations gliding on intersecting slip planes,**

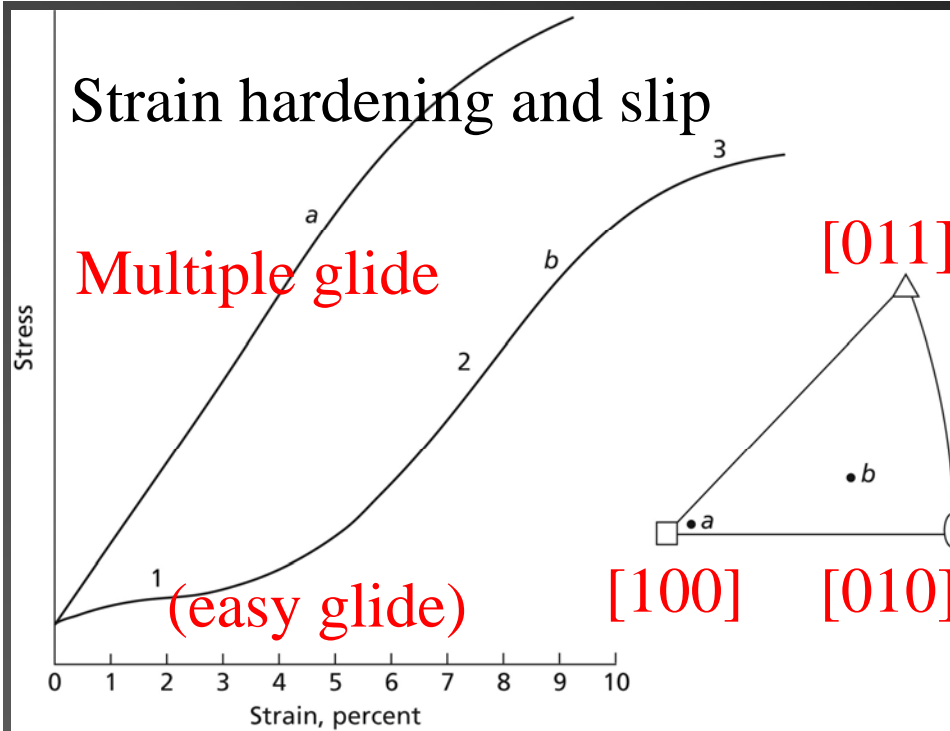


FIG. 5.17 Typical face-centered cubic single crystal stress-strain curves. Curve *a* corresponds to deformation by multiple glide from start of deformation; curve *b* corresponds to multiple glide after a period of single slip (easy glide). Crystal orientations are shown in the stereographic triangle

TABLE 5.3 The c/a Ratio for Hexagonal Metals.

Metal	c/a
Cd	1.886
Zn	1.856
Mg	1.624
Zr	1.590
Ti	1.588
Be	1.586

\Rightarrow Any plane contains a close-packed $\langle 111 \rangle$ direction can act as a slip plane.

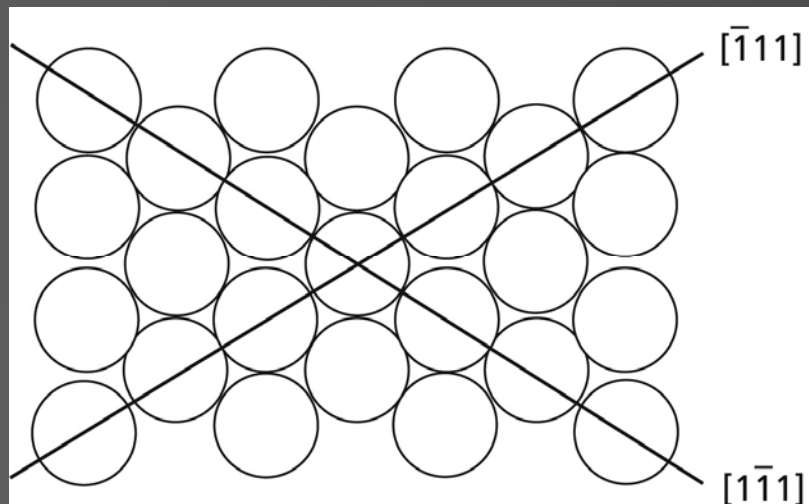


FIG. 5.19 The (110) plane of the body-centered cubic lattice

5.11 Cross-Slip (different from dislocation intersection)

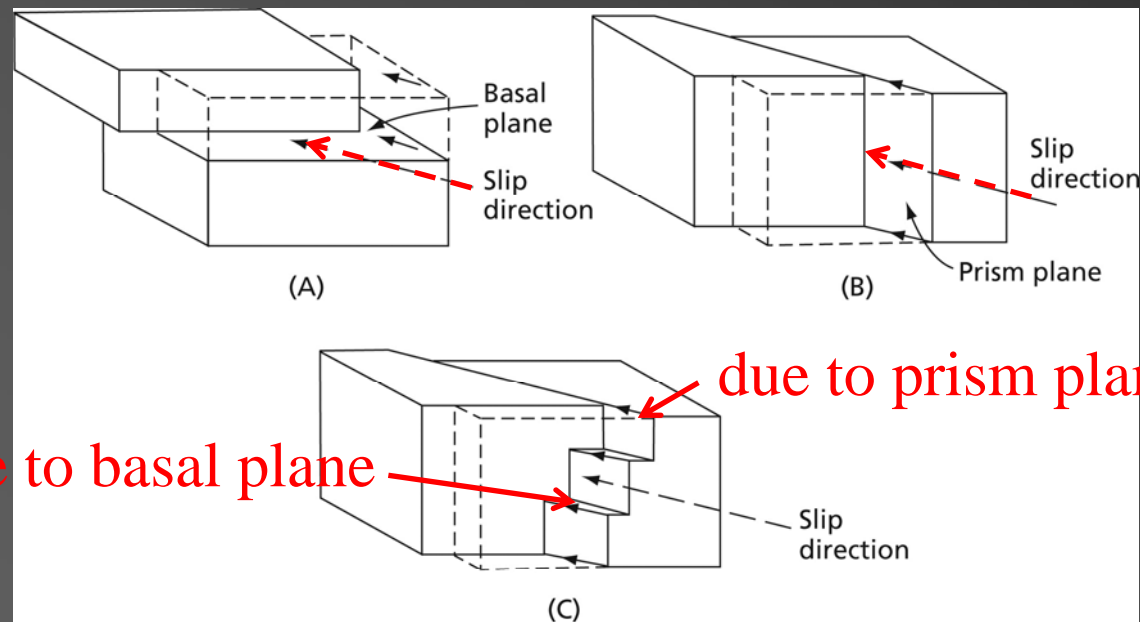
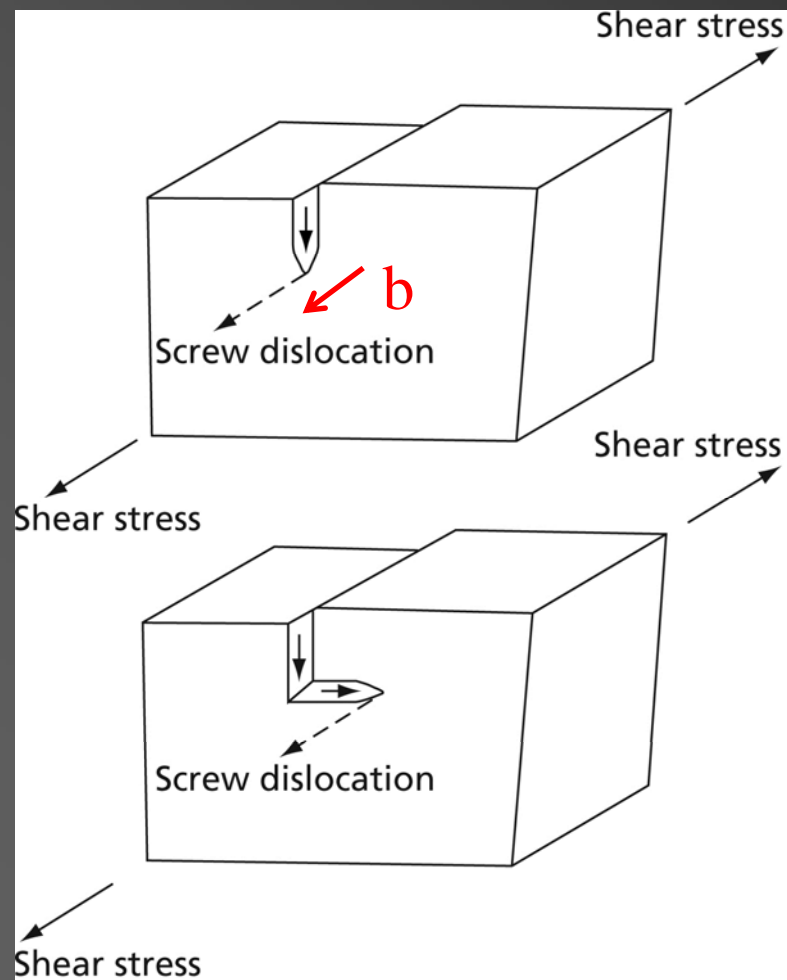


FIG. 5.20 Schematic representation of cross-slip in a hexagonal metal: **(A)** Slip on basal plane, **(B)** slip on prism plane, and **(C)** cross-slip on basal and prism planes



b: Burgers vector

- Screw dislocations move in different planes

FIG. 5.22 Motion of a screw dislocation during cross-slip. In the upper figure the dislocation is moving in a vertical plane, while in the lower figure it has shifted its slip plane so that it moves horizontally.

Prism plane $\{10\bar{1}0\}$

basal plane
(0001)

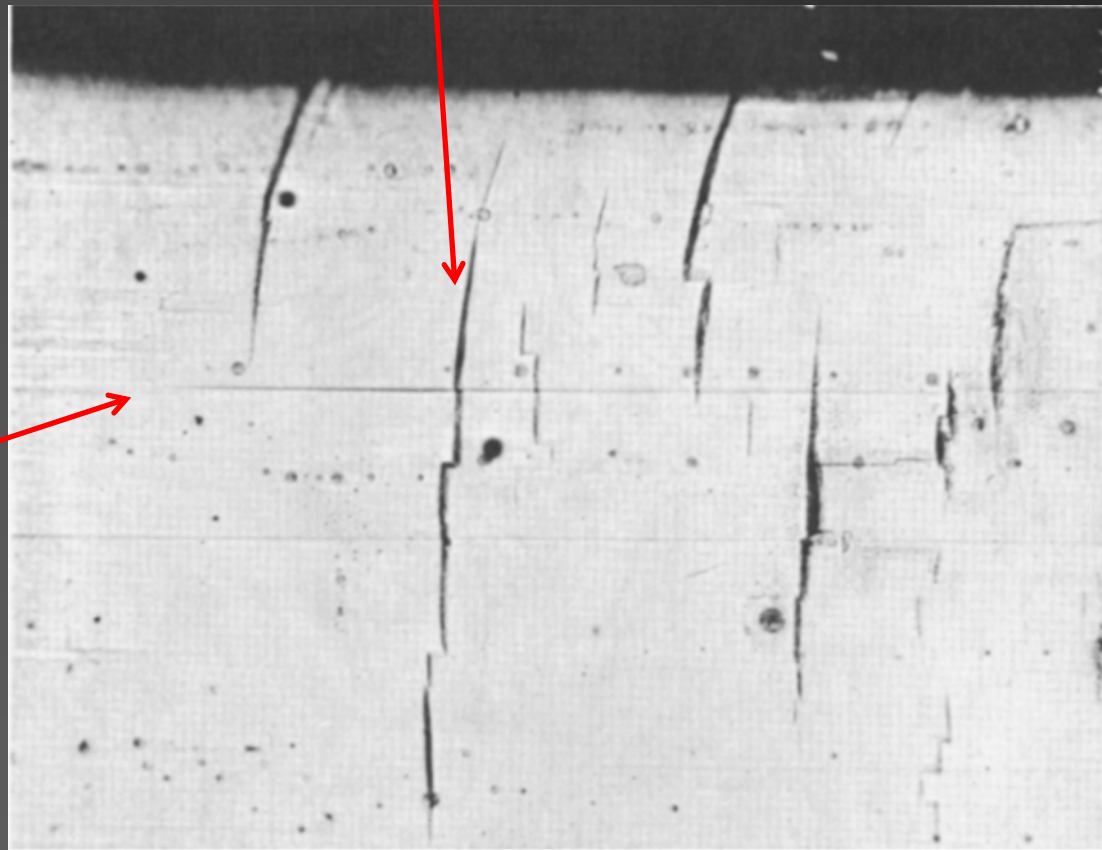
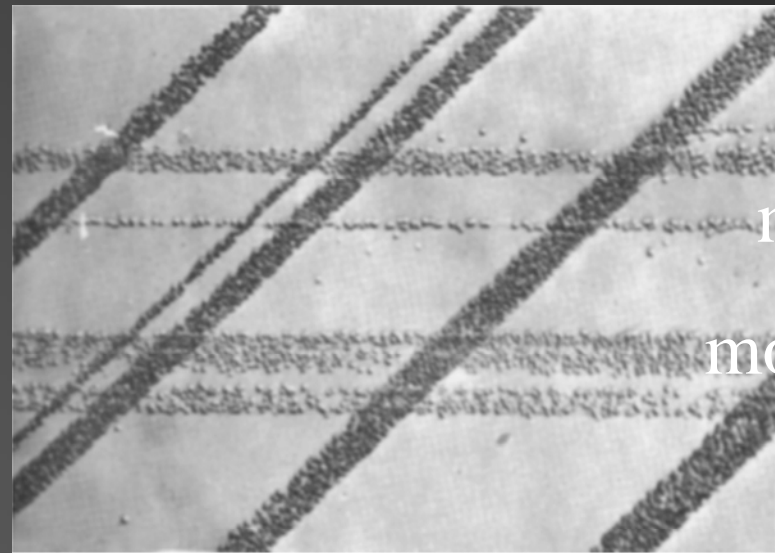


FIG. 5.21 Cross-slip in magnesium. The vertical slip plane traces correspond to the $\{10\bar{1}0\}$ prism plane, whereas the horizontal slip plane traces correspond to the basal plane (0002). $290\times$ (Reed-Hill, R. E., and Robertson, W. D., *Trans. AIME*, **209** 496 [1957].)

- In many HCP metals, no cross-slip can occur because the slip planes are parallel (not intersecting).
- A single crystal of Mg (HCP) can be stretched into a ribbon-like shape four ~ six times its original length.
- However, polycrystalline Mg shows limited ductilities (brittle).

5.12 Slip Bands:

Etch pits

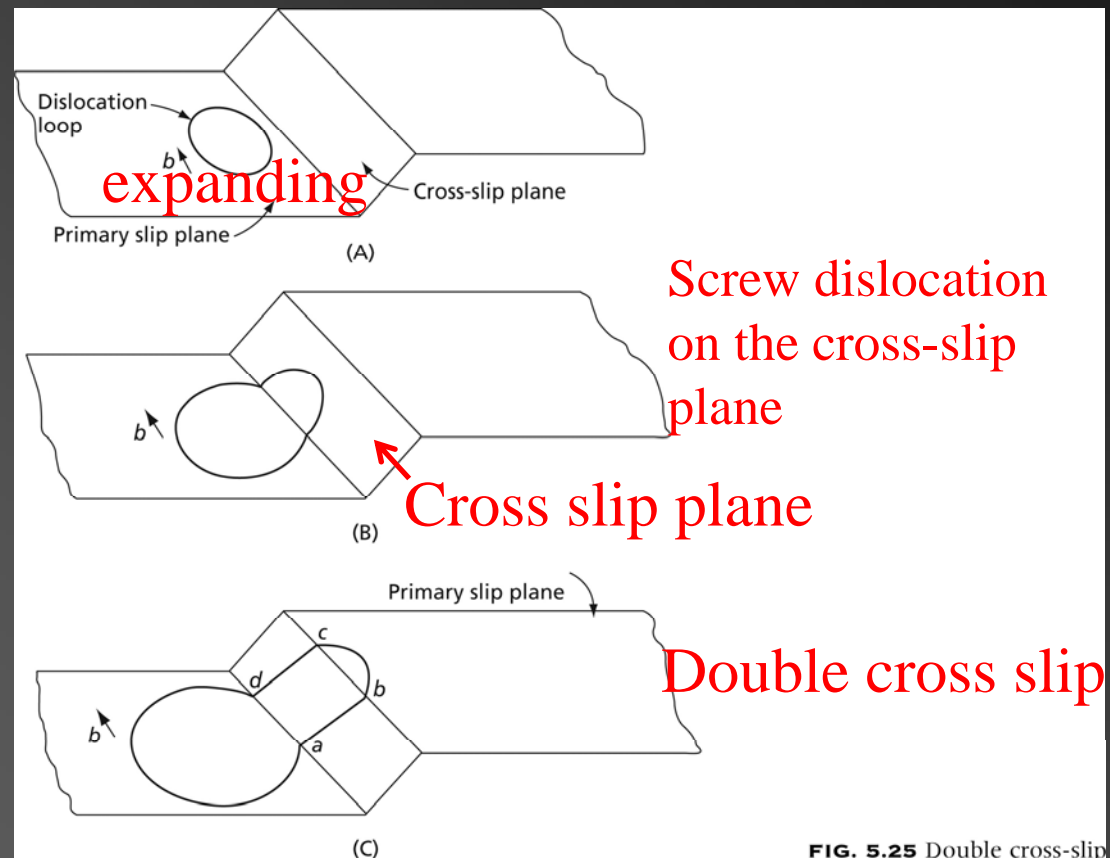


narrow
moderate

FIG. 5.24 Slip bands in LiF. Bands formed at -196°C and 0.36 percent strain (Reprinted with permission from J.J. Gilman and W.G. Johnson, *Journal of Applied Physics*, Vol. 30, Issue 2, Page 129, Copyright 1959, American Institute of Physics)

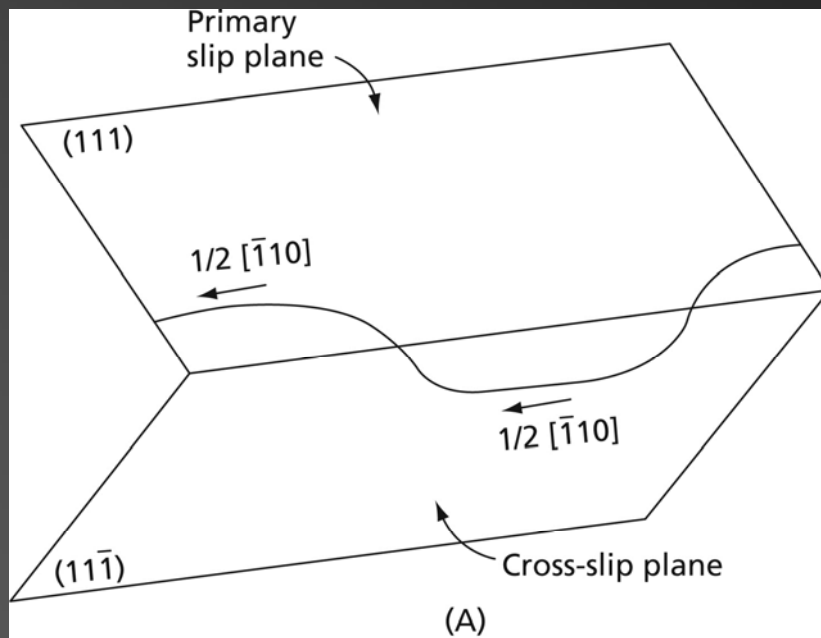
5.13 Double Cross-Slip:

- bc: dislocations can be created on the new slip plane.
- Similar to Frank-Read source.
- These freshly created dislocations **will not have enough time to become** pinned by impurity atoms.
- More probable than grown-in dislocations (slide 7).



5.14 Extended Dislocations and Cross-Slip

Common slip direction
[$\bar{1}10$]



$$\frac{1}{2} [\bar{1}10] = \frac{1}{6} [\bar{1}2\bar{1}] + \frac{1}{6} [\bar{2}11]$$

FIG. 5.26 The cross-slip of an extended dislocation

$$\frac{1}{6}[\bar{2}11] = \frac{1}{6}[\bar{1}21] + \frac{1}{6}[\bar{1}\bar{1}0]$$

Shockley partial Stair rod

Extended partials

$$\frac{1}{2}[\bar{1}10] = \frac{1}{6}[\bar{1}2\bar{1}] + \frac{1}{6}[\bar{2}11]$$

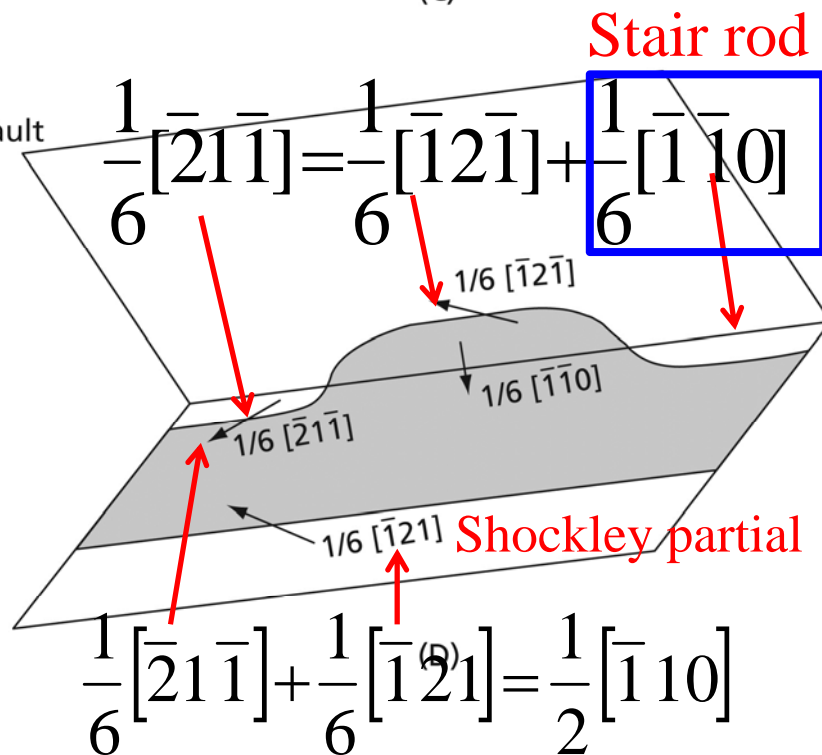
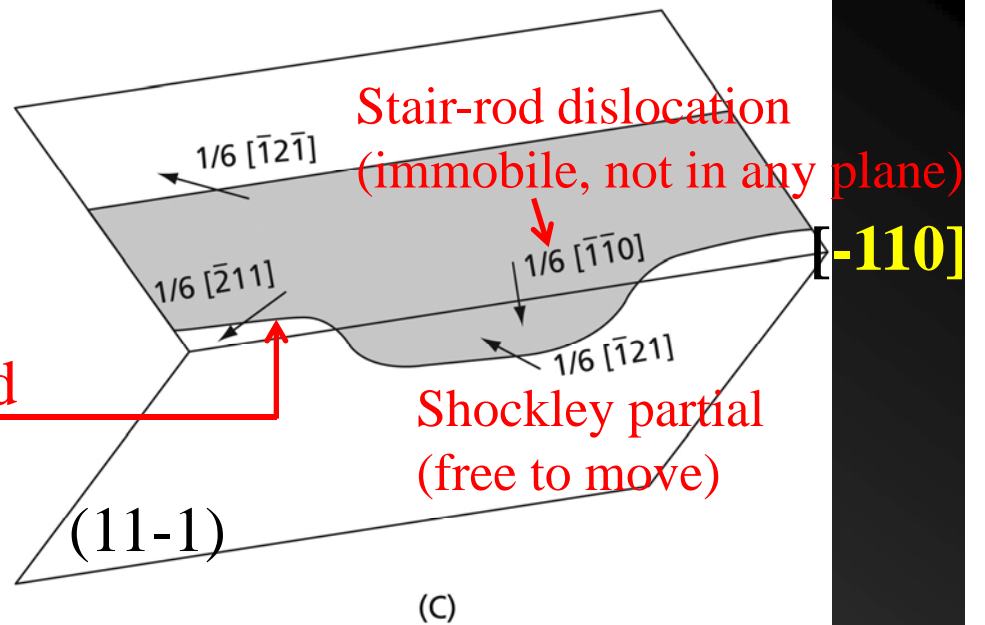
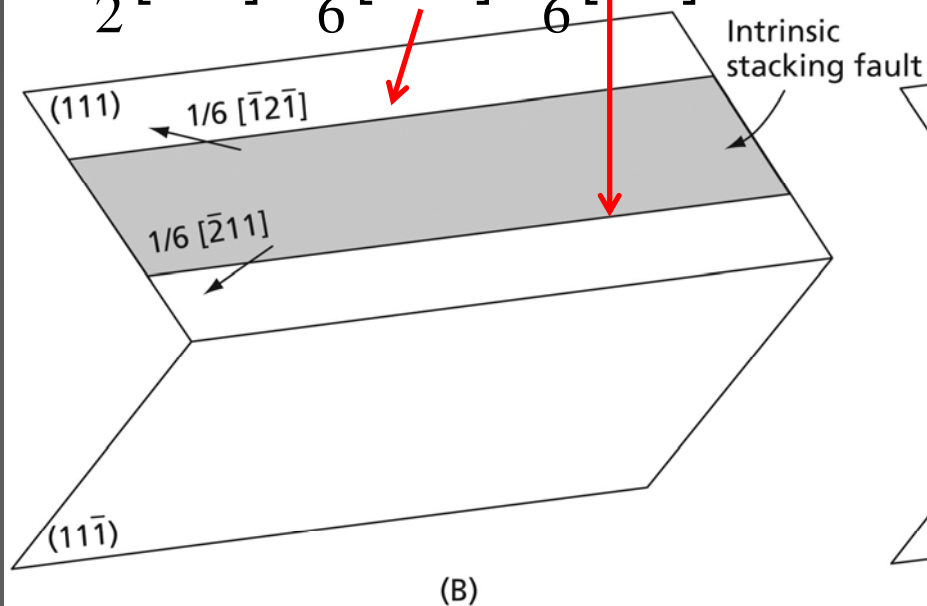


FIG. 5.26 The cross-slip of an extended dislocation

$$\begin{array}{ccc}
 & \boxed{(111)} & \boxed{\cancel{(11\bar{1})}} \\
 \frac{1}{2}[\bar{1}10] = & \frac{1}{6}[\bar{2}11] + \frac{1}{6}[\bar{1}2\bar{1}] \\
 & \downarrow & \downarrow \\
 & \boxed{\frac{1}{6}[\bar{1}\bar{1}0]} & \boxed{\frac{1}{6}[\bar{1}\bar{1}0]} \text{ Stair rod} \\
 & + & + \\
 \frac{1}{2}[\bar{1}10] = & \frac{1}{6}[\bar{1}21] & \frac{1}{6}[\bar{2}1\bar{1}] \\
 & \boxed{(11\bar{1})} &
 \end{array}$$

5.15 Crystal Structure Rotation during Tensile and Compressive Deformation

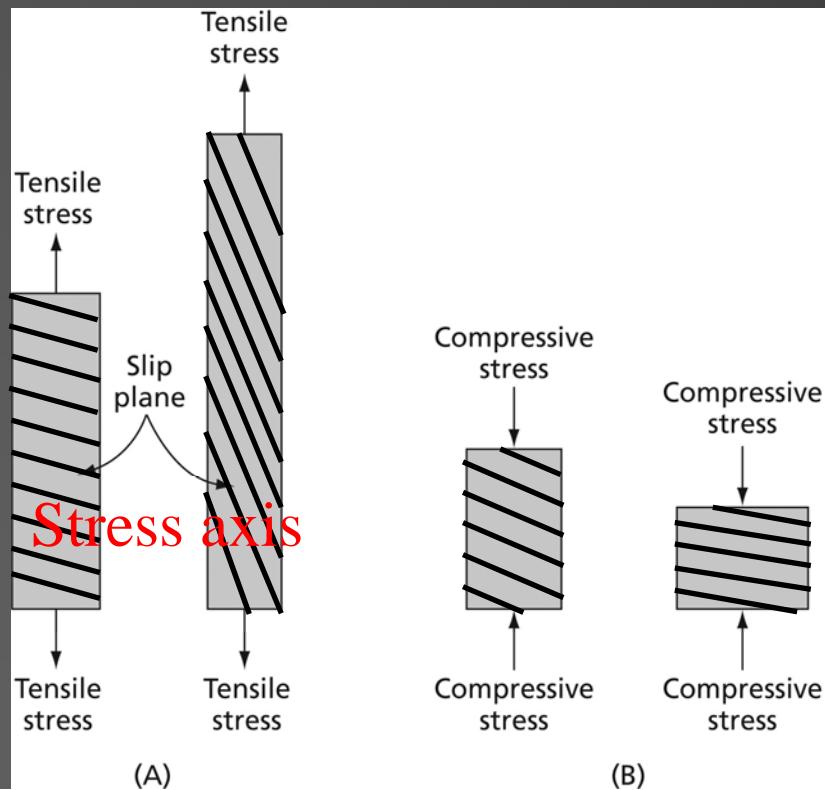


FIG. 5.27 Rotation of the crystal lattice in tension and compression

- In compression:
slip plane normal
// stress axis

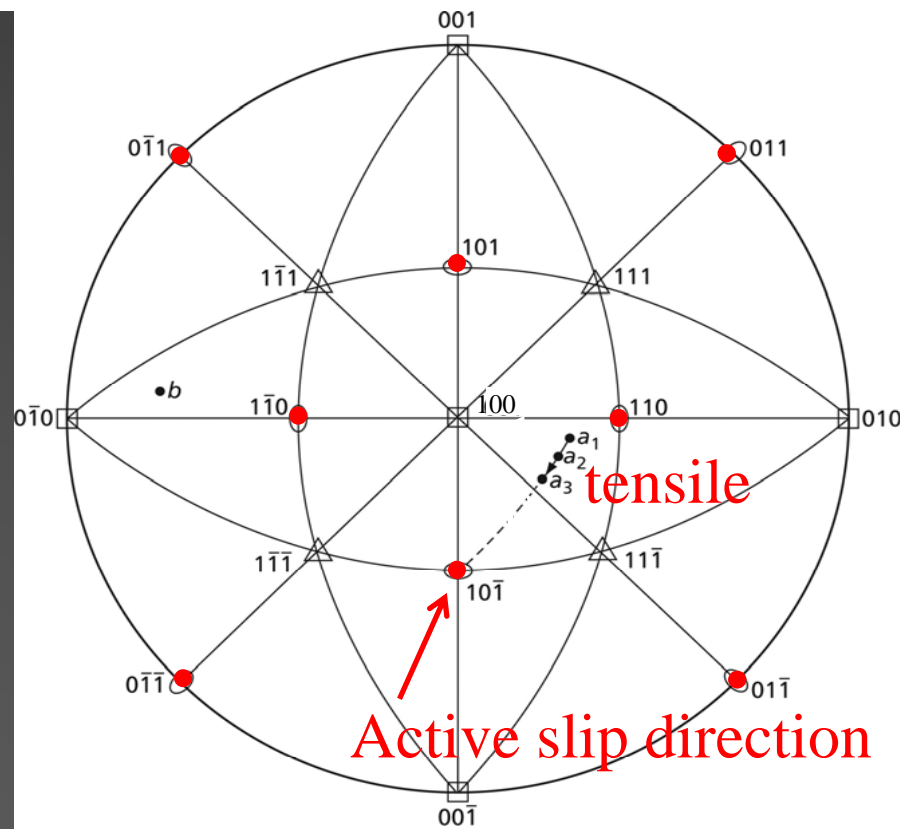


FIG. 5.28 In tension the lattice rotation is equivalent to a rotation of the stress axis (a) toward the slip direction. This stereographic projection shows this rotation in a face-centered cubic crystal

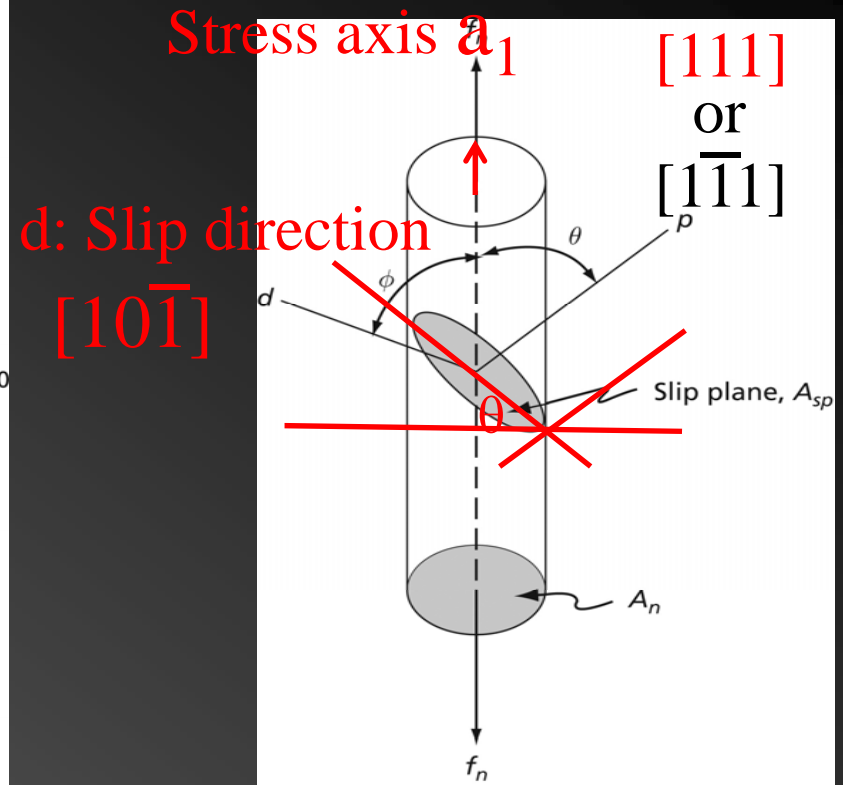


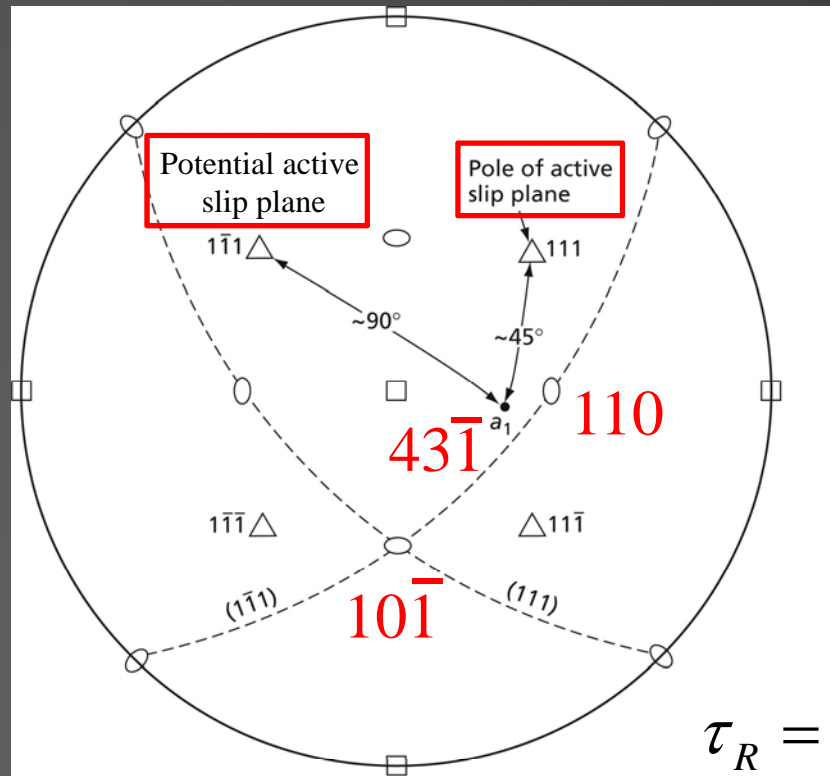
FIG. 5.14 A figure for the determination of the critical resolved shear stress equation

$$[43-1] \bullet [111] \Rightarrow \theta \sim 47^\circ$$

$$[43-1] \bullet [1-11] \Rightarrow \theta \sim 90^\circ$$

Primary slip system: $(111) [10\bar{1}]$

Cross slip system: $(\bar{1}\bar{1}1) [10\bar{1}]$



$$\tau_R = \sigma_A \cos \phi = \frac{f_n}{A_n} \cos \theta \cos \phi = \sigma \cos \theta \cos \phi$$

FIG. 5.29 The original stress axis orientation in Fig. 5.28 lies about 45° from the pole of the (111) plane and about 90° from the pole of $(\bar{1}\bar{1}1)$. These are the two slip planes that contain the active slip direction

$b [3-51]$

$b \bullet [1-1-1]; \theta \sim 47^\circ$

$b \bullet [111]; \theta \sim 96^\circ$

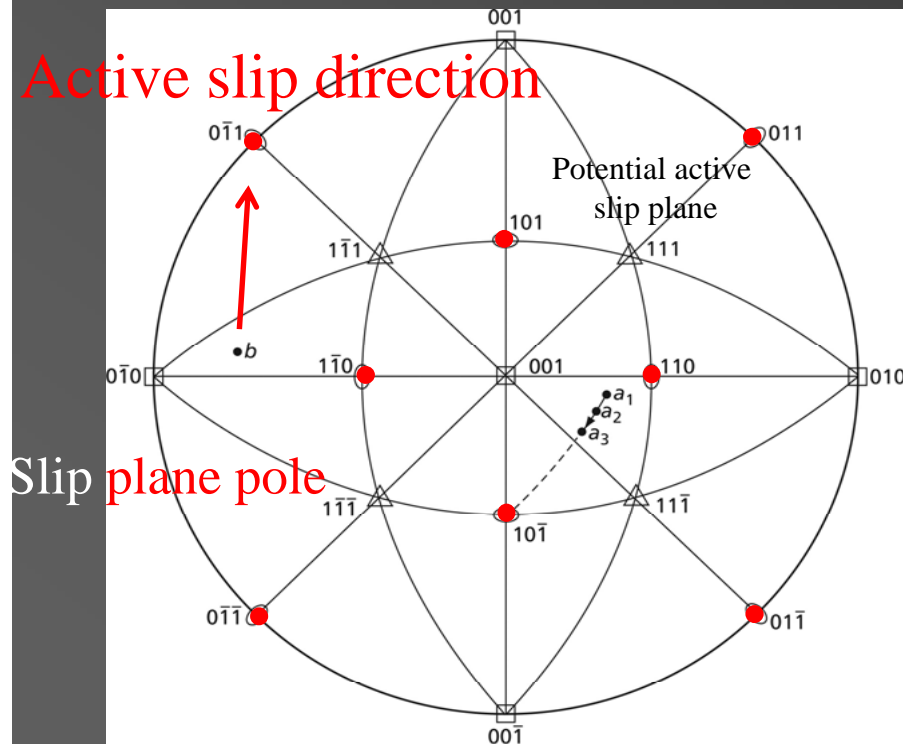
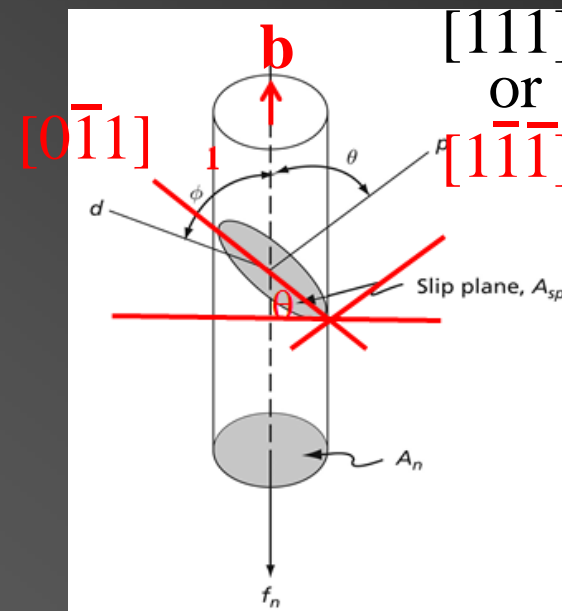


FIG. 5.28 In tension the lattice rotation is equivalent to a rotation of the stress axis (a) toward the slip direction. This stereographic projection shows this rotation in a face-centered cubic crystal

Primary slip system: $(1\bar{1}\bar{1}) [0\bar{1}1]$

Cross slip system: $(111) [0\bar{1}1]$



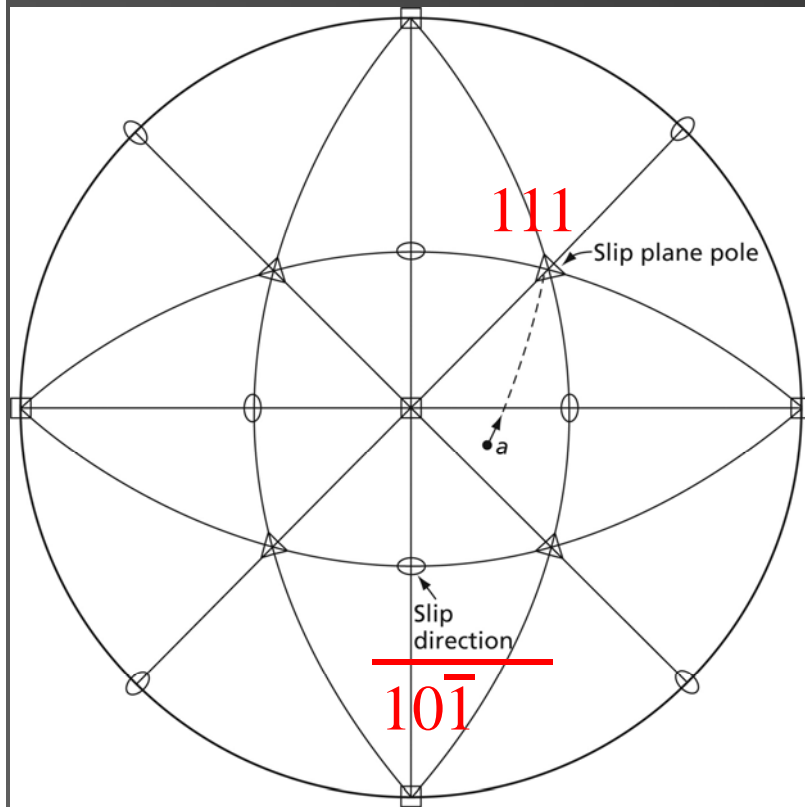


FIG. 5.30 In compression, the stress axis (a) rotates toward the pole of the active slip plane

d : Slip direction

$[10\bar{1}]$

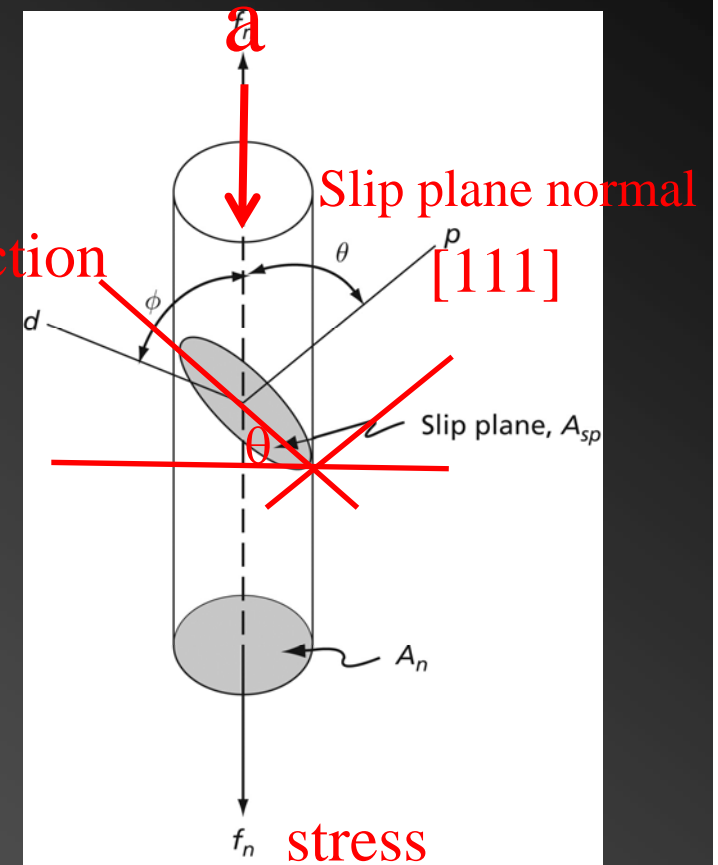


FIG. 5.14 A figure for the determination of the critical resolved shear stress equation

5.16 The Notation For The Slip Systems in The Deformation of FCC Crystals

Primary slip system: $(111) [10\bar{1}]$

Cross slip system: $(\bar{1}\bar{1}1) [10\bar{1}]$

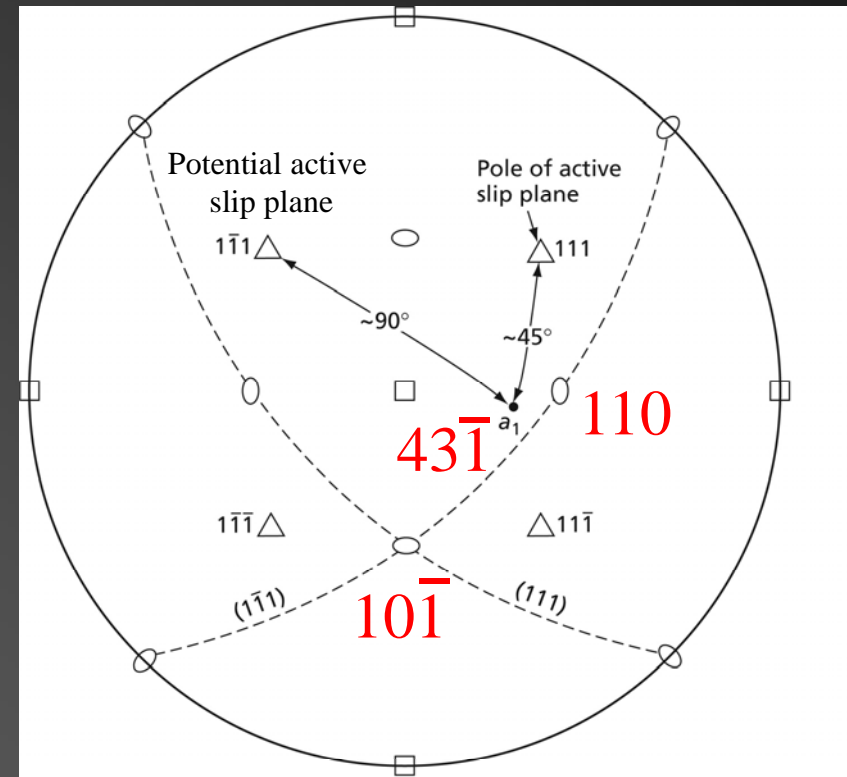
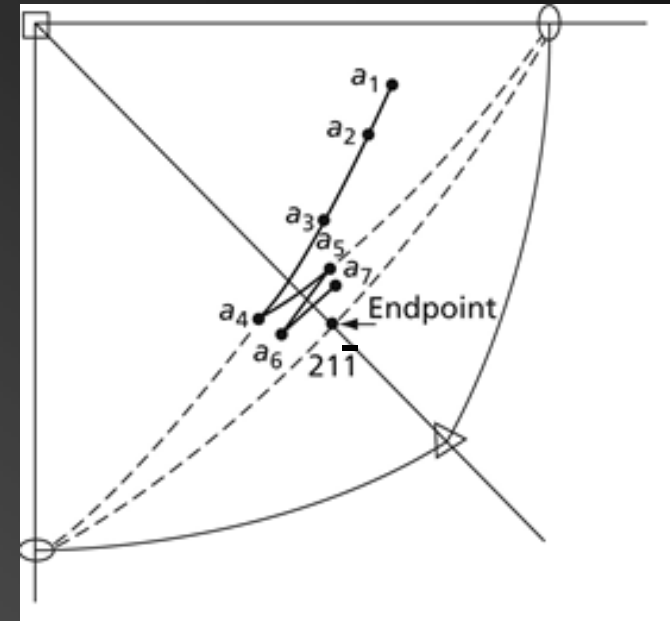
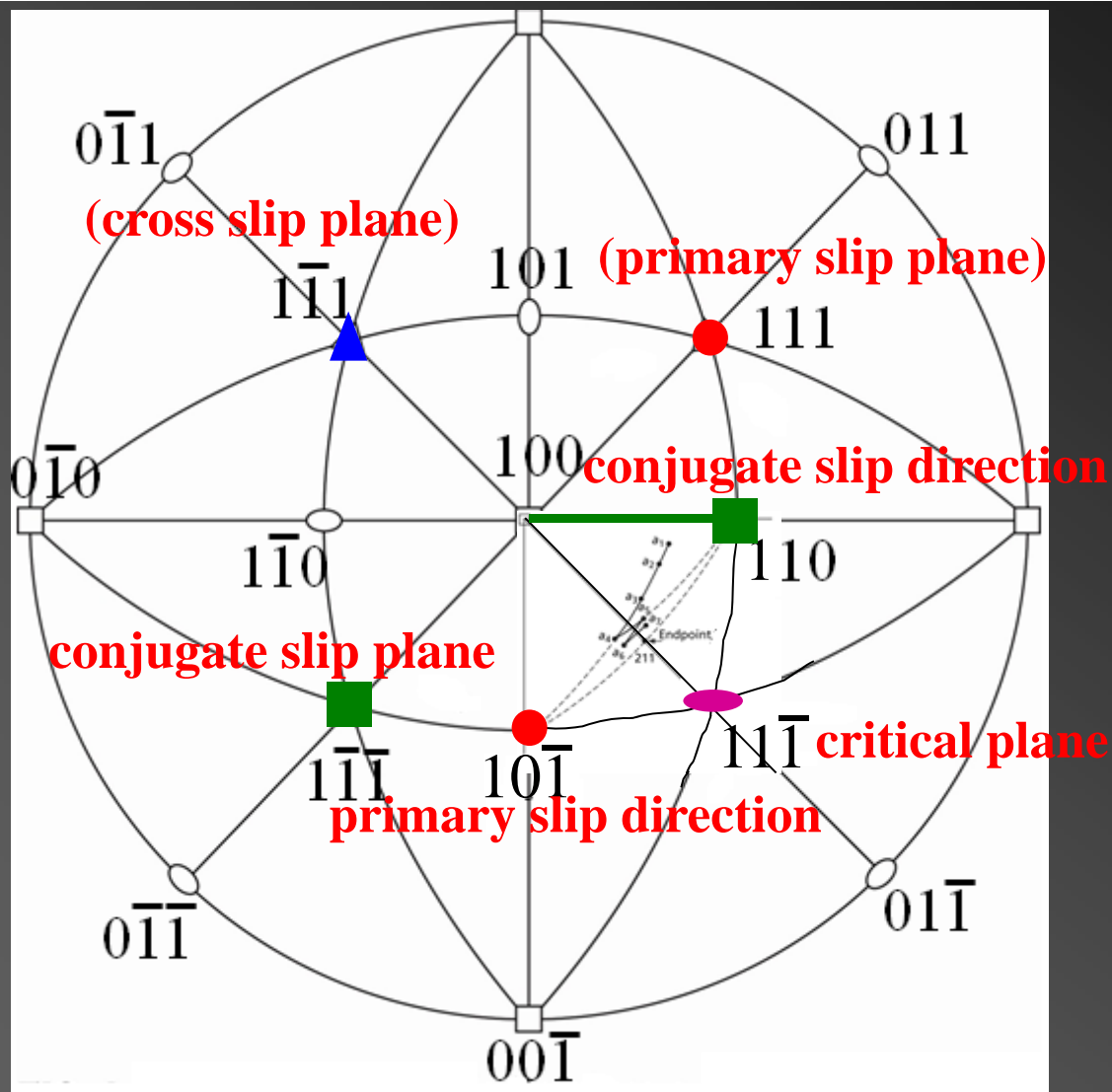


FIG. 5.29 The original stress axis orientation in Fig. 5.28 lies about 45° from the pole of the (111) plane and about 90° from the pole of $(\bar{1}\bar{1}1)$. These are the two slip planes that contain the active slip direction



- Conjugate slip system: happen once the rotation of the crystal out of its original stereographic triangle into the one adjoining it.
 \Rightarrow resolved shear stress is greater on the $(1\bar{1}\bar{1})[110]$ slip system.
 $\Rightarrow a_3 \rightarrow a_4$
- The crystal will continue to rotate with deformation occurring on alternating slip.

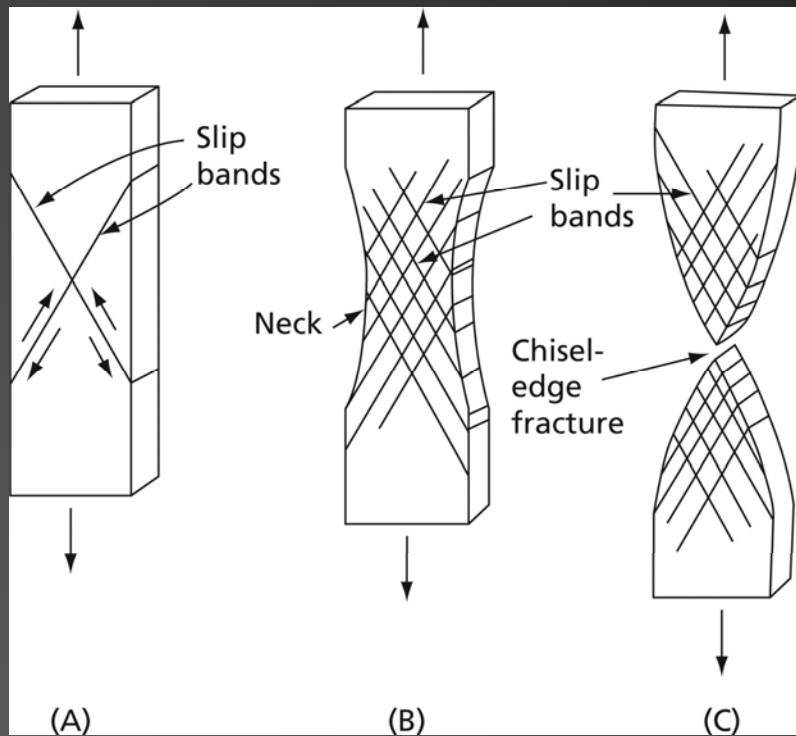


FIG. 21.3 (A) Crystal oriented for double slip. **(B)** Development of a neck. **(C)** Chisel edge fracture

Ductility: FCC > HCP > cubic

DISLOCATIONS AND MECHANICAL BEHAVIOUR OF MATERIALS p. 144

5.17 Work Hardening:

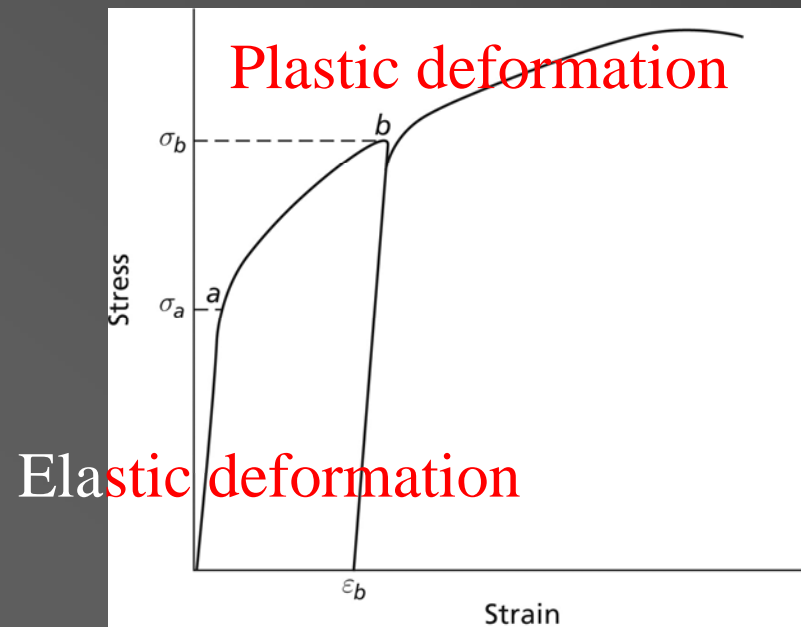


FIG. 5.32 Normally when a metal is deformed to a strain such as ϵ_b and then it is unloaded, it will not begin to deform until the stress is raised back to σ_b . The strain ϵ_b raises the flow stresses from σ_a to σ_b .

- Engineering stress and strain: expressed in terms of original sample dimension (A_0 , l_0).

$$\sigma_e = P/A_0 \text{ (P: load)}; \epsilon_e = (l_i - l_0) / l_0 = \Delta l / l_0$$

Figure 7.11 Typical engineering stress-strain behavior to fracture, point F . The tensile strength TS is indicated at point M . The circular insets represent the geometry of the deformed specimen at various points along the curve.

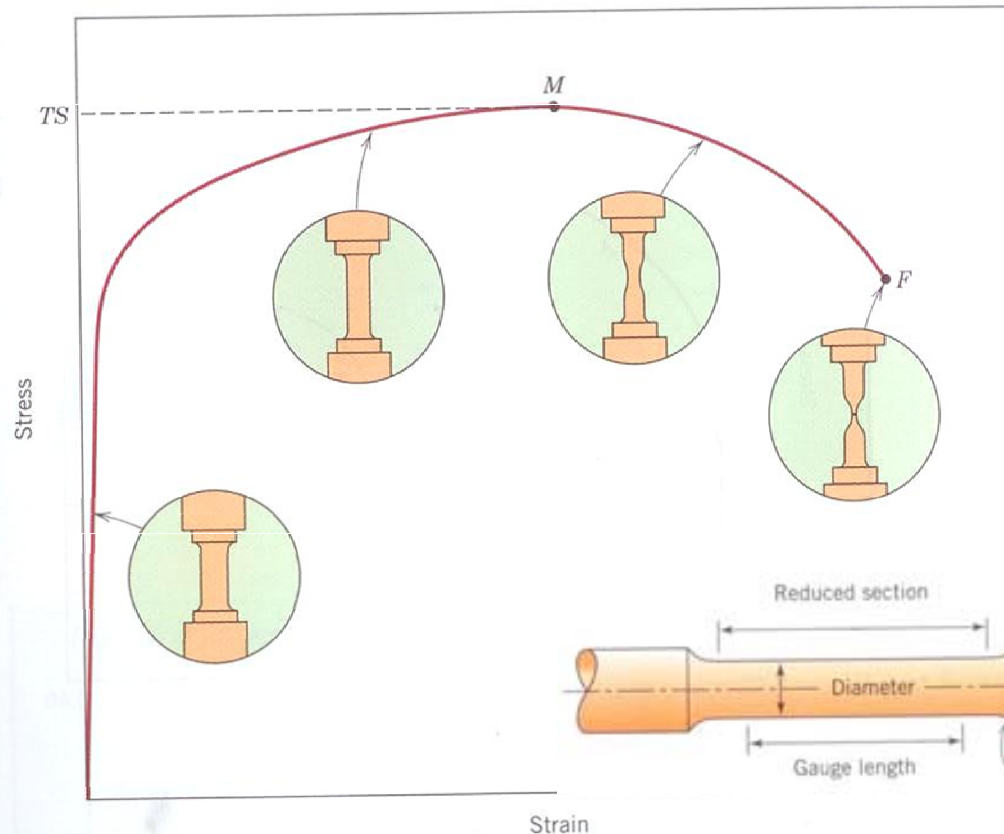
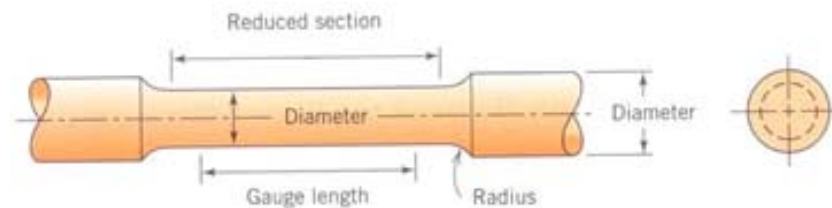


Figure 7.2 A standard tensile specimen with circular cross section.



$$\sigma_t = P/A_i \text{ (P: load)}; \epsilon_t = \Delta l/l_i \text{ (} l_i = l_0 + \Delta l \text{)}$$

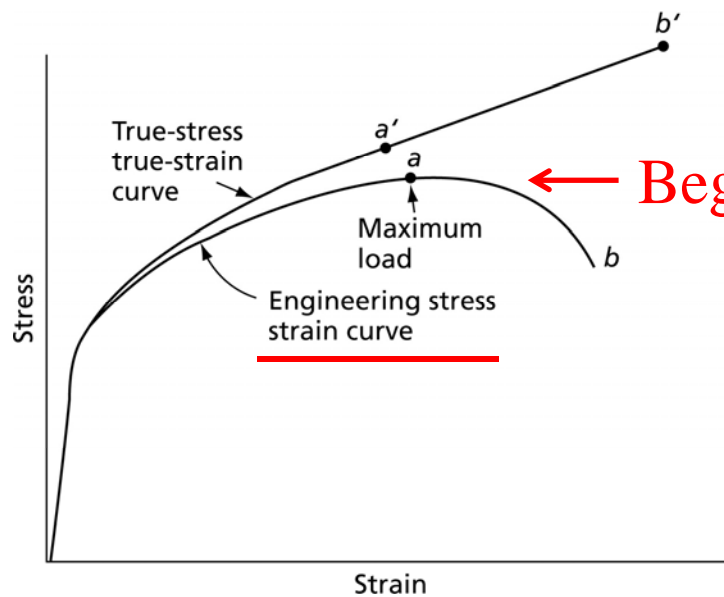


FIG. 5.33 A comparison between an engineering stress-strain curve and the corresponding true-stress and true-strain curve.

- The corrected $a \rightarrow a'$ takes into account the complex stress state within the neck region

- A true stress and strain curve has less practical meaning for the engineering application.
 - ⇒ Because you have to keep tracking the size for each strain, and what the engineers care most is how strong the materials are and when they are going to fail.

$$\sigma_t = P/A_i; \quad \varepsilon_t = \Delta l/l_i \qquad \sigma_e = P/A_0; \quad \varepsilon_e = \Delta l/l_0$$

$$\sigma_t = \frac{P}{A_i} = \frac{Pl_i}{A_i l_i} = \frac{Pl_i}{A_0 l_0} = \frac{P}{A_0} \frac{l_0 + \Delta l}{l_0} = \sigma_e (1 + \varepsilon_e) \qquad l_i = l_0 + \Delta l$$

σ_t : true stress;

σ_e : engineering stress;

P : load

ε_t : true strain;

ε_e : engineering strain;

Δl : increase in length.

$$\begin{aligned} \varepsilon_t &= \int_{l_0}^{l_i} \frac{dl}{l} = \ln \frac{l_i}{l_0} = \ln \frac{l_0 + \Delta l}{l_0} \\ &= \ln(1 + \varepsilon_e) \end{aligned}$$

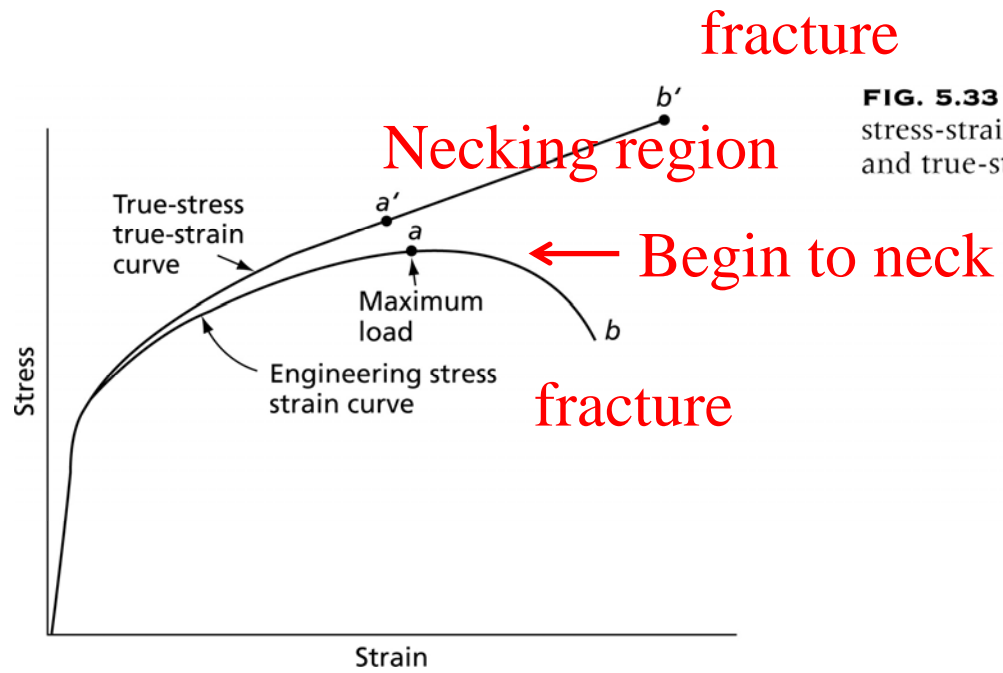
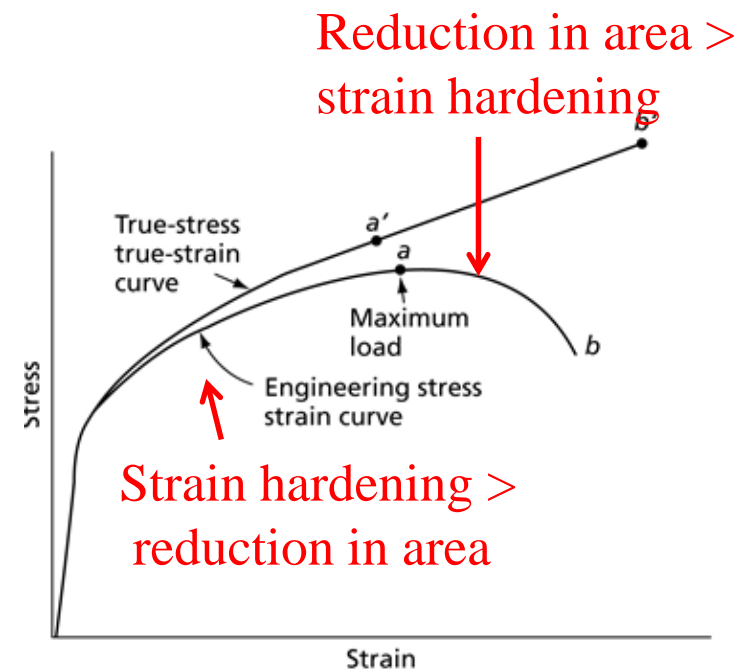


FIG. 5.33 A comparison between an engineering stress-strain curve and the corresponding true-stress and true-strain curve.

5.18 Considere's Criterion



loading

Area reduction

$$P = \sigma_t A_i \Rightarrow dP = \boxed{A_i d\sigma_t} + \boxed{\sigma_t dA_i} = 0 \Rightarrow d\sigma_t = -\sigma_t \frac{dA_i}{A_i}$$

Strain hardening

$$dV = d(A_i l_i) = A_i dl_i + l_i dA_i = 0 \Rightarrow \frac{dA_i}{A_i} = -\frac{dl_i}{l_i} = -d\varepsilon_t$$

$$\Rightarrow \sigma_t = -\frac{\frac{d\sigma_t}{\frac{dA_i}{A_i}}}{\frac{dl_i}{l_i}} = \frac{d\sigma_t}{d\varepsilon_t} : \text{Considere's criterion}$$

5.19 The Relation Between Dislocation Density And The Stress (Experimentally Observed)

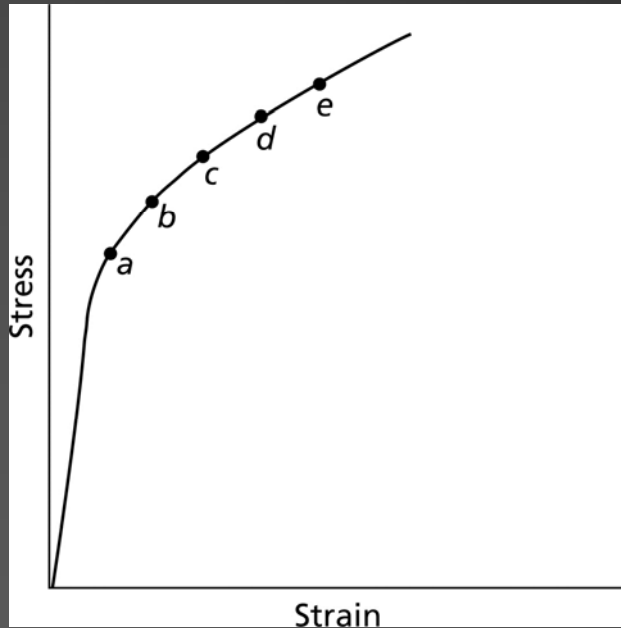


FIG. 5.34 To determine the variation of the dislocation density with strain during a tensile test, a set of tensile specimens are strained to a number of different positions along the stress-strain curve, such as points a to f in this diagram. These specimens are then sectioned to obtain transmission electron microscope foils

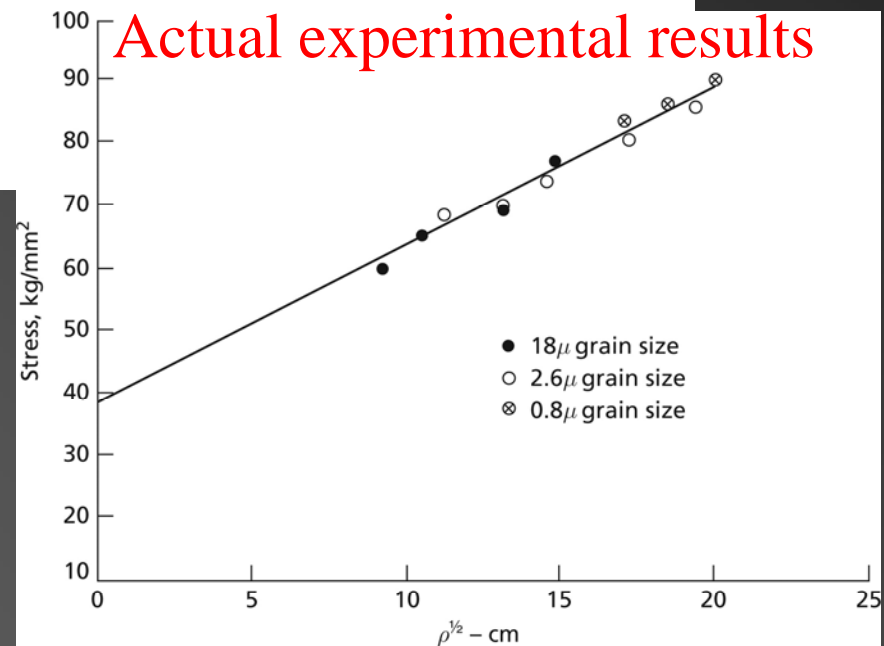


FIG. 5.35 The variation of the flow-stress σ with the square root of the dislocation density $\rho^{1/2}$ for titanium specimens deformed at room temperature, and at a strain rate of 10^{-4} sec⁻¹ (After Jones, R. L., and Conrad, H., *TMS-AIME*, **245** 779 [1969].)

$$\sigma = \sigma_0 + k\rho^{1/2}$$

σ : flow stress
 ρ : measured dislocation density
 σ_0 : extrapolated to zero

$$\tau = \tau_0 + k\rho^{1/2}$$

τ : flow stress
 ρ : measured dislocation density
 τ_0 : extrapolated to zero

- If ρ is zero, the metal **could not be deformed**.
 $\Rightarrow \sigma_0$ and τ_0 are best considered as **convenient constants rather than as simple physical properties**.

5.20 Taylor's Relation

$$\tau = \mu\gamma = \mu b / (2\pi r) = \alpha \mu b / r$$

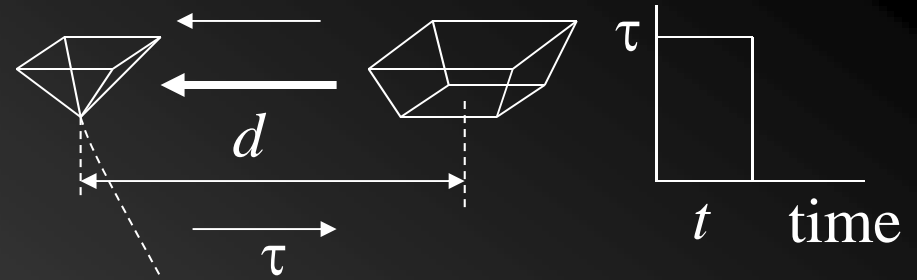
$$r \propto \rho^{-1/2}$$

$$\tau = \alpha \mu b / \rho^{-1/2} = \alpha \mu b \rho^{1/2} = k \rho^{1/2} \quad \text{where } k = \alpha \mu b$$

5.21 Dislocation velocity

- Dislocation velocity (v)

$$v = d/t$$



1. From experimental data => Johnston and Gilman found

$$\ln v \propto \ln \tau$$

power law: $v = (\tau/D)^m$

D : the stress yields at $v = 1 \text{ cm s}^{-1}$; τ : applied shear stress

m : exponent; function of purity, temp. etc.

2. Temperature dependence of v t_f : time of flight between obstacles => $\ln v \propto 1/T$ (phonon effect)

3. Combine 1 & 2: single expression

$$v = \underbrace{f(\sigma)}_{\text{Stress dependence term}} \underbrace{e^{-E/kT}}_{\text{Temperature dependence term}} \quad 25^\circ\text{C} > T > -50^\circ\text{C}$$

E : activation energy;

T : absolute temperature;

k : Boltzmann's constant

Stress
dependence term

Temperature
dependence term

5.23 The Orowan Equation (Strain Rate)

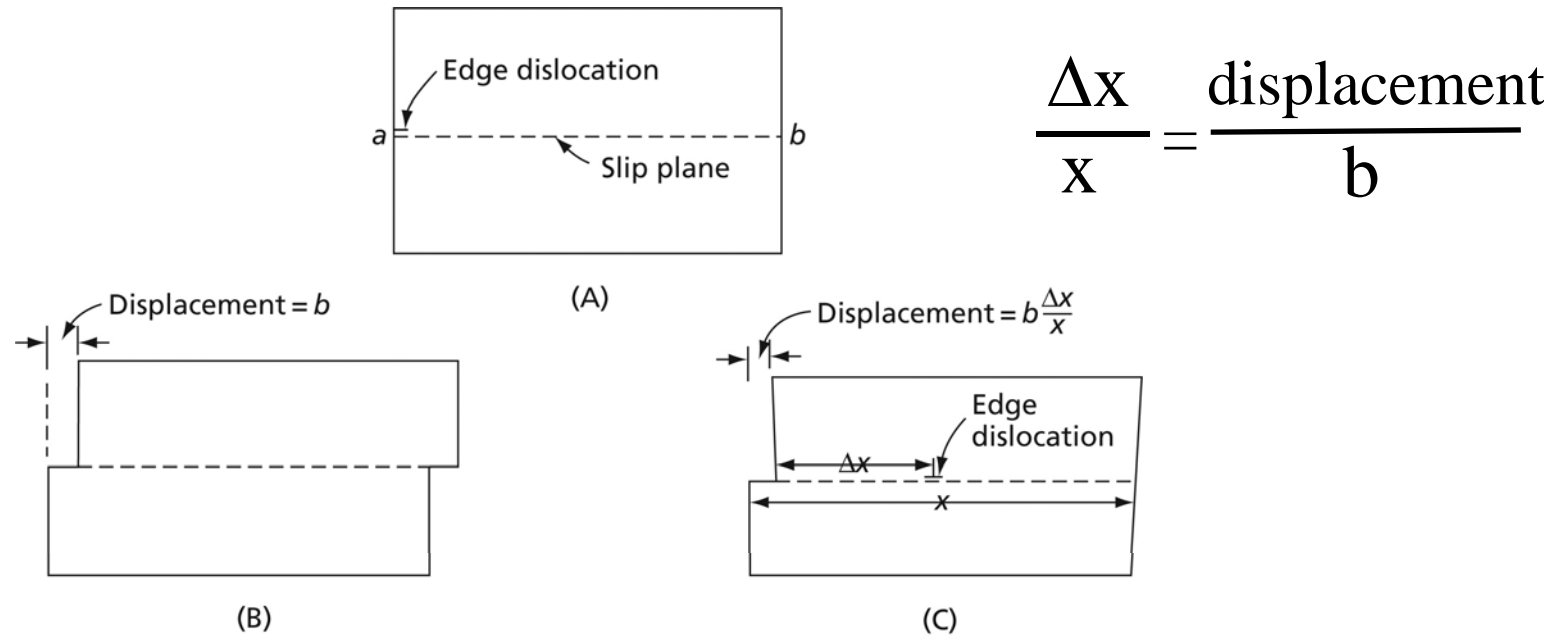


FIG. 5.36 The displacement of the two halves of a crystal is in proportion to the distance that the dislocation moves on its slip plane

- relation between the velocity (v) of the dislocations and the applied strain rate ($\dot{\epsilon}$).

In (c): Shear by an amount =
$$\frac{b \Delta x}{x} = \frac{b \Delta A}{A}$$

$$\Delta\gamma \propto (b\Delta x/x)/x = \rho b\Delta x \text{ (because } (1/x^2) = \rho)$$

ρ : the dislocation density

Shear strain rate: $\frac{\Delta\gamma}{\Delta t} = \dot{\gamma} = \frac{\rho b\Delta x}{\Delta t} = \rho b\bar{v}$

$$\dot{\varepsilon}$$

Tensile strain rate: $\dot{\varepsilon} = \frac{1}{2} \dot{\gamma} = \frac{1}{2} \rho b\bar{v}$



Schmid orientation factor

5.22 The Discontinuous Nature of Dislocation Movement

- In real crystal, there are a lot of obstacles in lattice
 - => the movement of a dislocation is not smooth and continuous, but rather it occurs in steps.
 - => Moves rapidly for a short distance; it stops and waits at an obstacle while eventually it passes; it moves rapidly again to the next obstacle.

